表1　我が国の主要な小児がん臨床研究グループ

小児がん臨床研究グループ名	対象病型	実施中の試験数	ホームページなどの情報
日本小児白血病・リンパ腫研究グループ（JPLSG）	白血病，悪性リンパ腫など	11	http://jplsg.jp
日本横紋筋肉腫研究グループ（JRSG）	横紋筋肉腫	4	文献1
日本ユーイング肉腫研究グループ（JESS）	Ewing肉腫	1	文献2
日本神経芽腫研究グループ（JNBSG）	神経芽腫	2	http://www.jnbsg.jp/
日本小児肝癌スタディグループ（JPLT）	肝芽腫など	1	http://home.hiroshima-u.ac.jp/jpltstudy/index.html
日本ウィルムス腫瘍スタディグループ（JWiTS）	Wilms腫	1	文献3
日本小児脳腫瘍コンソーシアム（JPBTC）	髄芽腫など	2	http://www.es-bureau.org/contents/consortium/

表2　現在進行中の小児がん関連臨床試験一覧

病型	試験名	研究グループ	試験ID*
急性リンパ性白血病	・乳児急性リンパ性白血病に対する早期同種造血幹細胞移植療法の有効性に関する後期第Ⅱ相試験（MLL03）	JPLSG	
	・小児フィラデルフィア染色体陽性急性リンパ性白血病（Ph＋ALL）に対するimatinib mesylate第Ⅱ相臨床試験（Ph＋ALL04）	JPLSG	C000000290
急性骨髄性白血病	・小児急性前骨髄急性白血病（APL）に対する多施設共同後期第Ⅱ相臨床試験（AML-P05）	JPLSG	UMIN000000645
	・小児急性骨髄性白血病（AML）に対する多施設共同後期第Ⅱ相臨床試験（AML-05）	JPLSG	UMIN000000511
	・ダウン症候群に発症した小児急性骨髄性白血病に対するリスク別多剤併用化学療法の後期第Ⅱ相臨床試験（AML-D05）	JPLSG	UMIN000000989
悪性リンパ腫	・ALCL99（未分化大細胞型リンパ腫を対象としたヨーロッパとの共同研究）	JPLSG	
	・小児成熟B細胞性腫瘍に対する多施設共同後期第Ⅱ相臨床試験（B-NHL03）	JPLSG	C000000317
	・進行期小児成熟B細胞性腫瘍に対する顆粒球コロニー刺激因子（G-CSF）の一次的予防投与の有用性に関する無作為割付比較試験（B-NHL03 G-CSF）	JPLSG	UMIN000000675
	・小児リンパ芽球型リンパ腫stage Ⅰ/Ⅱに対する多施設共同後期第Ⅱ相臨床試験（LLB-NHL03）	JPLSG	
	・小児リンパ芽球型リンパ腫stage Ⅲ/Ⅳに対する多施設共同後期第Ⅱ相臨床試験（ALB-NHL03）	JPLSG	
血球貪食症候群	・Treatment Protocol of the Second International HLH Study（HLH-2004）	JPLSG	
横紋筋肉腫	・横紋筋肉腫低リスクA群患者に対する短期間VAC 1.2療法の有効性および安全性の評価第Ⅱ相臨床試験	JRSG	
	・横紋筋肉腫低リスクB群患者に対する短期間VAC 2.2/VA療法の有効性および安全性の評価第Ⅱ相臨床試験	JRSG	
	・横紋筋肉腫中間リスク群に対するiVAC療法の有効性および安全性に関する多施設共同研究	JRSG	
	・進行性・転移性横紋筋肉腫に対する自家造血幹細胞救援療法を併用した大量化学療法第Ⅱ床試験	JRSG	
Ewing肉腫	・限局性ユーイング肉腫ファミリー腫瘍に対する集学的治療法の第Ⅱ相臨床試験	JESS	
神経芽腫	・進行神経芽腫に対する遅延局所療法早期第Ⅱ相臨床試験	JNBSG	UMIN000000973
	・高リスク神経芽腫に対する標準的治療の後期第Ⅱ相臨床試験	JNBSG	UMIN000001044
肝癌	・小児肝癌に対するJPLT-2治療プロトコール臨床第Ⅱ相試験	JPLT	UMIN000001116
Wilms腫	・本邦における腎腫瘍に対する病期別統一プロトコール治療の完遂率と有効性の評価（JWiTS-2）	JWiTS	
髄芽腫またはテント上PNET	・小児髄芽腫/PNETに対する多剤併用化学療法と減量放射線療法の第Ⅱ相試験	JPBTC	UMIN000000545
	・乳幼児髄芽腫/PNETに対する多剤併用化学療法および大量化学療法の第Ⅱ相試験	JPBTC	UMIN000000546

*：試験IDは以下のサイトで検索した．
UMIN臨床試験登録システム（UMIN CTR）：http://www.umin.ac.jp/ctr/index-j.htm
財団法人日本医薬情報センター（JAPIC）臨床試験データベース：http://www.clinicaltrials.jp/user/cte_main.jsp
国立保健医療科学院 臨床研究〔試験〕情報検索：http://rctportal.niph.go.jp/
国立がんセンターがん情報サービス：http://ganjoho.ncc.go.jp/professional/med_info/clinical_trial/ct0120.html

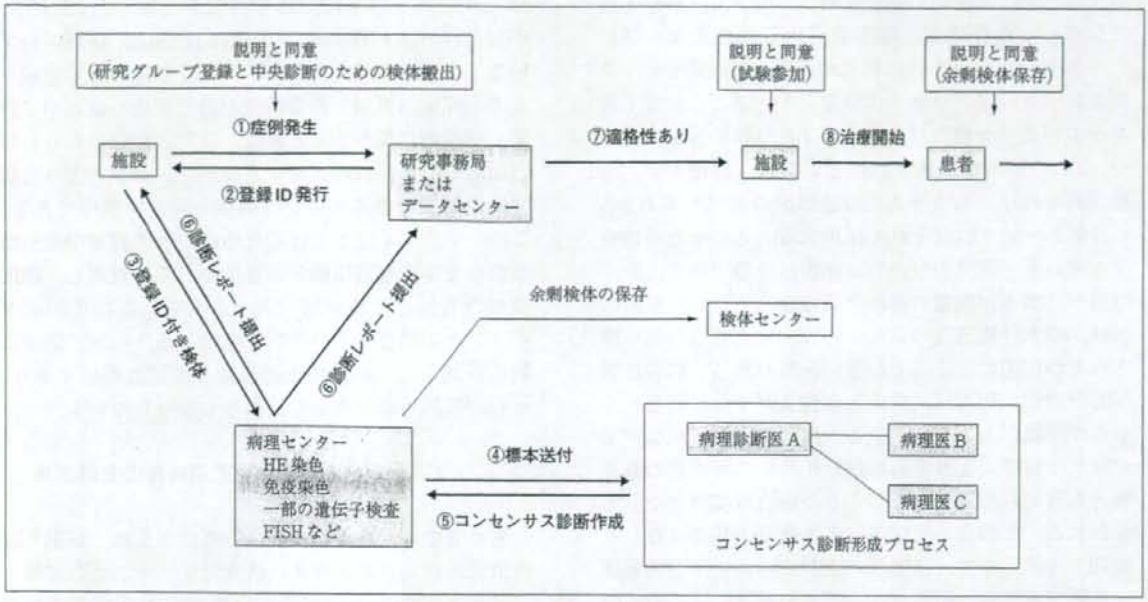

図1　小児がんの臨床試験登録と病理中央診断システム　我が国の小児がん臨床試験で一般的に行われている情報と検体の流れ，その中での病理中央診断システムと余剰検体保存の関連を示す．症例が発症した場合，施設は研究事務局あるいはデータセンターに登録申請を行い登録IDの発行を受ける(①②)．施設は患者検体に登録IDを付けて病理センターに送付する(③)．病理センターは必要な染色等を行った後，指定した病理医に標本を送付する(④)．病理医間でコンセンサス診断を作成し，病理センターを経由して診断レポートを施設ならびにデータセンターに送付する(⑤⑥)．試験参加の適格性の判断が施設に伝えられ治療が開始する(⑦⑧)．なお，このプロセスの中で，患者あるいは代諾者に対して，研究グループ登録と中央診断への検体搬出，試験参加，余剰検体保存，それぞれについて説明が行われ同意が取得される．

小児がんは稀少であるため，スタディクエスチョンを解決するためには，ある程度の症例数が必要となる場合がある．また，新しい臨床試験計画を独自で作成するための国内のエビデンスに乏しい場合もある．そのような場合には，海外で実施されている臨床試験に参加することも視野に入れた研究が展開されている．JPLSGが実施する試験のうち2件(ALCL99およびHLH-2004)は海外との共同研究である．

近年，臨床試験を実施するにあたっては試験内容を登録し公開することを義務づけようとする動きが高まってきている．その理由は，一般にネガティブデータは論文等で公表されない傾向があり，より透明性を確保することを目的としたものである．数年前に欧米の主要雑誌が協調し，事前に試験を登録して公開していない場合は論文掲載を行わない旨の発表を行った．以後，我が国でも登録制度と情報検索のシステムが整備されつつある．上記の研究グループが実施する臨床試験の多くが登録されており概要を検索することができる(**表2**脚注)．

Ⅱ．臨床研究グループと病理中央診断

さて，上記の各臨床研究グループが実施する臨床試験の多くで病理中央診断が実施されている．研究グループごとに複数の専任病理医を定めているが，その多くを日本病理学会小児腫瘍組織分類委員会のメンバーが担当している．病理中央診断の手順は試験ごとに作成される実施計画書に具体的に記載されているが，基本的には以下のごとくである(**図1**)．まず，試験に該当すると思われる患者が発生した場合，主治医は患者あるいは代諾者に，推測される疾患に該当する臨床試験への参加ならびに中央診断のための検体送付について説明し同意を得る．採取される検体やその処理方法は試験ごとに定められているが，病理中央診断の場合は，HE染色標本は必須で，それ以外に融合遺伝子検索などのため未固定検体の提出を求めているものもある．症例によっては免疫染色用に5～10枚程度の未染薄切標本提出を求めることもある．中央診断の

方法は一般には複数の病理医のコンセンサス診断としてレポートを作成し，標本を提出した施設ならびにデータセンター（または研究事務局）に連絡する．コンセンサス形成プロセスは研究グループごとに若干異なっている．一般には，例えば3名の診断医がいる場合，2名の診断が一致すればその診断を採用する，意見が異なれば，もう一人別の診断医の意見を求め2名の診断が一致すればそれを採用する，といった手法を採っている．意見が分かれる理由は多様である．多くの場合，標本が微量のため全体像がみえない，組織の挫滅，標本作成過程の何らかの理由による質の悪い標本などが原因になることが多いと思われる．純粋に学問的な理由，例えば，疾患概念がまだ十分に固まっておらず主観が入る余地がある．概念が確立されているが新たな指標によりさらに細分化される可能性のある場合も考えられるが，そのような場合は案外少ないと思われる．このような理由による意見の相違はむしろ歓迎すべきもので，多数例の検討でのエビデンス蓄積が重要であるし，研究グループとの連携による中央診断システムはそれらの解明を可能にしうるものである．

Ⅲ．小児腫瘍組織分類委員会の役割

日本病理学会小児腫瘍組織分類委員会は，日本小児外科学会，日本小児科学会からの協同の要請により設置され，1975年の小児腫瘍組織分類図譜第1篇小児肝癌，腎芽腫，神経芽腫群腫瘍の発刊をはじめとして，「癌取扱い規約」に相当する小児がんに関する分類図譜を編集・発行し，我が国における小児がんならびに関連疾患に関わる情報提供を通じて，疾患概念の認識と診断の標準化を目指すことを主たる業務としている．分類図譜はWHO分類や国際的に認知されている学術団体などが公表する最新分類に準拠し，我が国で普及させるための適切な形式に編集して定期的に発行している．以前は，「小児腫瘍組織分類図譜」という名称を使用していたが，2001年発行の版からは「小児腫瘍組織カラーアトラス」と名称変更しかつモダンなデザインの外観としている．

前述のごとく，当委員会のメンバーの多くが小児がんの臨床研究グループの中央診断担当医として参画してきたが，小児腫瘍組織分類委員会としてのまとまった活動ではなく，むしろボランティア的な活動であった．また，臨床研究グループに登録される症例は限られたものであるため，我が国の全体像を把握することはできないといった問題も明らかとなった（ただし，小児悪性リンパ腫の90％程度はJPLSGに登録されていると予想される）．これらの問題を解決する手段として小児腫瘍組織分類委員会が研究グループの中央診断に積極的に関与すると共に，研究に登録されない症例についても，いわばコンサルテーションのような形で中央診断できるシステム構築を現在考慮中である．このシステムを立ち上げるために，小児腫瘍中央診断委員会を小児腫瘍組織分類委員会内部に設置し，症例受付から始まる新診断システム考案，各臨床研究グループとの調整などの活動を開始した．なお，臨床試験に参加しない症例の追跡調査は重要な課題であり，それが実施可能な体制の整備をも目指している．

Ⅳ．診断後の余剰検体や研究用検体の有効活用

言うまでもないが，正確な診断がなされ，詳細な臨床情報が付いた患者検体は研究用リソースとして極めて価値が高い．患者検体を収集する方法を考えた場合，上記のような中央診断システムを利用することが効率的かつ現実的な方法である．実際には中央診断後の残余検体（余剰検体）について患者あるいは代諾者の同意の下に研究用リソースとして保存している場合が多い（図1）．さらには，これら検体は可能な限り一箇所に集約する動きにあり，国立成育医療センター研究所や千葉県がんセンター研究所などが検体センターとして機能している．このような中央診断後の余剰検体のみならず，初めから研究用に採取され使用される検体もある．これらの検体の残余分も貴重なリソースである．現在，臨床試験に関わる余剰検体が順調に集積されてきているが，問題点としては，このような貴重なリソースをどのような取り決めで使用していくかについてのコンセンサスが未だ形成されていない点である．米国最大の小児がん研究グループであるChildren's Oncology Group（COG）では，中央診断システムならびに検体センターをコロンバスにあるNationwide Children's Hospital一箇所に集約し，また，配分ルールもグループ内でのコンセンサスとして決定している．それらも参考にしながら我が国でも共有リソースの使用ルールを決める必要がある．

Ⅴ．米国における小児がん臨床試験と中央診断，検体保存

米国では，数年前に幾つか個別に活動していた小児がん研究グループがCOGという一つの大きな枠組み

の中で活動するようになった．各種レベルの臨床試験の推進のみならず，中央診断システム構築，余剰検体の保存と活用，長期フォローアッププログラムの開発など多角的な活動を展開している．前述のようにCOGにおける中央診断と検体保存のセンターはNationwide Children's Hospital（Columbus Children's Hospitalから最近名称変更，http://www.nationwidechildrens.org）内のBiopathology Center（http://www.biopathologycenter.org）に全て集約されている．そもそもは，同病院病理のStephen J. Qualman博士が始めた事業であるが，現在は極めて高度に発展したシステムとなっている（Qualman博士は昨年引退され，Nilsa C. Ramirez博士が後継者として就任している）．米国には1980年代より全米のがんを対象としたCooperative Human Tissue Network（CHTN，http://www.chtn.nci.nih.gov）がNCIの資金により構築されており，1991年にはすでにPediatric Divisionが出来上がってColumbus Children's Hospitalがセンターとして指名されている．CHTNは検体を収集して中央に保存するというシステムではなく，検体は各施設で保存し情報だけを中央に集めて共有し，必要に応じて配分するというバーチャルバンキングシステムである．現在は，小児がんの多くがCOGの中で診断され治療されるため検体もCOG経由でBiopathology Centerに集められるが，スタディに参加しない症例の検体も有効活用できるシステムとなっている．

COGが行う臨床試験に関わる病理中央診断についても，いったん全ての検体がCOGに集められ，必要な染色等を行ったうえで病型別に定められた病理医に送付されるという形態をとっている．なお，Biopathology CenterにはVIPER（Virtual Imaging for Pathology Education & Research，http://viper.epn.osc.edu/viper/）と呼ぶバーチャルスライドユニットが存在する．オハイオ大学のスーパーコンピュータと共同で開発しており，診断そのもの，診断の標準化および教育といった目的のために活用されている．Biopathology Centerは小児がんのような稀少疾患の研究を推進するための一つの究極の形かもしれない．

Ⅵ．小児がん登録

疾病の基本情報の収集や分析といった地道な活動は我が国では大変立ち遅れている．がん登録もその一つで，昨年成立したがん対策基本法にも盛り込まれず，付帯事項として記載され，がん対策推進計画の中で計画の一つとして表現されるにとどまった．小児がん登録も言わずもがなの状況であり，推進計画の中には言葉としては出てくるが，小児がんを計画に盛り込んでいる自治体は皆無である．地域がん登録は2008年5月現在35道府県市で実施されているがその中で小児がん登録を意識的に位置づけているところは大阪府のみである．ただし，大阪府の場合も意識の高い小児科医の献身的な努力によって支えられているのが現状である．このような状況の中，小児がんの診療に関わる医師たちが学会ベースで小児がんの全数把握に取り組む計画を立案中である．日本小児外科学会（http://www.jsps.gr.jp/public/registration.htm），日本小児血液学会（http://www.jsph.info/osirase/JSPH-touroku.html）ならびに日本小児がん学会（http://www.ccaj-found.or.jp/jspo/general/index.htm）はそれぞれ独自に小児がん登録を実施してきたが，登録率の向上，国際比較の必要性などを考慮し，日本小児がん学会が関連学会と連携して従来より精度の高い小児がん登録を実施する計画を立てている．小児がんの国際比較には，International Classification of Diseases for Oncology 3rd Edition（ICD-O）に基づいたInternational Childhood Cancer Classification 3rd Edition（ICCC-3）[4]が使用されているため，日本小児がん学会が収集する情報を最終的にICCC-3に従って編集できるように現在使用中の登録票ならびに登録方法を改訂中である．

小児がん患者の生存率が70%ないし80%となり長期にわたる生存が期待できる状況となって，小児がん登録に求める役割に変化が起こりつつある．すなわち，二次がん発生やその他の各種晩期合併症の発生をも把握できるシステムづくりを目指すべきとの意見が広まりつつある．国と自治体が連携して推進する地域がん拠点病院構想や学会主導のがん治療認定医制度や認定施設制度の定着と広がりの中で，小児がんについても成人と同じように診療体制の整備が必要であり，小児がん登録もその中に組み込まれるべきものであると考える．

おわりに

我が国における小児がんに関する質の高い臨床研究は始まったばかりと言える．病理医はこのような研究の枠組みの中でかなり重要な役割を演じる必要がある．数年間の経験からは，ある種の小児がん病型では

中央診断と施設診断の間で不一致率が10%を超えるものもあった．これらの情報をいかに現場に還元していくかは中央診断を担当する病理医ならびに小児腫瘍組織分類委員会に課せられた課題であると考える．精度の高い診断を達成するためには，医療現場の病理医の協力が必須であり，今後，学会や書物を通じて小児がんの臨床研究における病理医の活動を広く宣伝，紹介してゆきながら理解を得てゆきたいと考えている．コロンバスのBiopathology Centerの現責任者Ramirez博士との会話では，検体配分についても彼女が大変強い権限をもっていることがわかった．診断のみならず検体保存や配分に際しても病理医は強い指導力を発揮すべきなのだと思う．今後，我が国ではがん診療拠点病院のネットワークが構築されてゆくが，それらの病院では院内がん登録が義務づけられる．そのような場面でも病理医は指導的な役割を発揮するのだと思う．その際，小児がんにもご留意いただけると大変ありがたいと思う次第である．

文　献

1) 森川康英：小児横紋筋肉腫に対する中央病理診断及び遺伝子診断に基づく臨床試験の確立と新規治療法開発に関する研究，がん研究助成金報告書（http://ganjoho.ncc.go.jp/pro/mhlw-cancer-grant/2005/keikaku/17-13.pdf）
2) 国立がんセンターがん対策情報センター：がん情報サービス，小児がんシリーズの冊子「小児のユーイング肉腫について」（http://ganjoho.ncc.go.jp/public/qa_links/brochure/child.html）
3) 越永従道，七野浩之，福澤正洋：小児腎腫瘍における治療成績と方針．小児科診療 2005，68：1643-1650
4) International Classification of Childhood Cancer, 3rd ed., SEER International Classification of Childhood Cancer（http://seer.cancer.gov/iccc/）を参照．また，United Kingdom Association of Cancer Registriesよりダウンロード可能（http://82.110.76.19/coding/iccc3.pdf）

In Vitro Gene Delivery by pDNA/Chitosan Complexes Coated with Anionic PEG Derivatives that Have a Sugar Side Chain

Mayu Hashimoto,[1] Yoshiyuki Koyama,[2] and Toshinori Sato*[1]
[1]*Faculty of Science and Technology, Keio University, 3-14-1 Hiyoshi, Kouhoku-ku, Yokohama 223-8522*
[2]*Department of Home Economics, Otsuma Women's University, Chiyoda-ku, Tokyo 102-8357*

(Received December 10, 2007; CL-071368; E-mail: sato@bio.keio.ac.jp)

The cationic pDNA/chitosan complexes were coated with anionic poly(ethylene glycol) derivatives (PEG-A/Cs) that have a sugar side chain. Coating the pDNA/chitosan complex with maltose- or lactose-modified PEG-A/C (Mal–PEG-A/C or Lac–PEG-A/C, respectively) greatly promoted their stability in water and transfection efficiency in vitro.

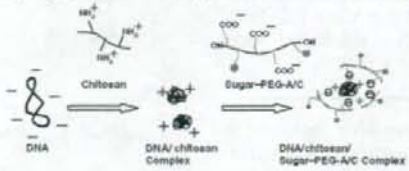

REPRINTED FROM

Chemistry Letters

Vol.37 No.3 2008 p.266–267
CMLTAG
March 5, 2008

The Chemical Society of Japan

Published on the web (Advance View) February 2, 2008; doi:10.1246/cl.2008.266

In Vitro Gene Delivery by pDNA/Chitosan Complexes Coated with Anionic PEG Derivatives that Have a Sugar Side Chain

Mayu Hashimoto,[1] Yoshiyuki Koyama,[2] and Toshinori Sato*[1]
[1]*Faculty of Science and Technology, Keio University, 3-14-1 Hiyoshi, Kouhoku-ku, Yokohama 223-8522*
[2]*Department of Home Economics, Otsuma Women's University, Chiyoda-ku, Tokyo 102-8357*

(Received December 10, 2007; CL-071368; E-mail: sato@bio.keio.ac.jp)

We developed pDNA/chitosan complexes coated with sugar-modified PEG-A/Cs, which are poly(ethylene glycol) derivatives with a side chain of carboxylic acid and sugar. The cationic pDNA/chitosan complexes were coated with anionic sugar-modified PEG-Cs, and anionic ternary complexes were formed. Coating the pDNA/chitosan complexes with maltose- or lactose-modified PEG-A/C (Mal–PEG-A/C or Lac–PEG-A/C, respectively) greatly promoted their stability in water and transfection efficiency in vitro.

A number of cationic polymers have been developed to deliver exogenous genes into cells. Chitosan is a naturally occurring polysaccharide showing low cytotoxicity, biocompatibility, and biodegradability,[1] and is often employed as a gene carrier. Sato et al. reported that DNA/chitosan complexes were uptaken into tumor cells, but not into blood monocytes.[2] Plasmid DNA (pDNA)/chitosan also showed high-level transfection efficiency both in vitro[3] and in vivo.[4] However, the stability of pDNA/chitosan complexes in water was low by self-aggregation and BSA-induced aggregation. To improve the stability and cell-specificity of the pDNA complexes, lactose- and mannose-modified chitosans have been developed as gene carriers.[5]

Poly(ethylene glycol), PEG, has been widely employed for drug delivery systems to prevent non-specific interaction with serum protein and cells. Conjugation of PEG to pDNA/polyethyleneimine (PEI) complexes resulted in a prolonged circulation time after intravenous injection.[6] The conjugation of PEG to pDNA/chitosan complexes increased the stability in water.[7] However, such a conjugation of PEG to the pDNA/chitosan complexes did not enhance their transfection efficiency.

In this study, we employed PEG derivatives with carboxylic acid and sugar moieties (sugar–PEG-A/Cs) as side chains to coat DNA/chitosan complexes. Anionic sugar–PEG-A/Cs form ternary complexes electrostatically with cationic pDNA/chitosan complexes (Figure 1). Sugar–PEG-A/Cs have been employed to coat pDNA/PEI complexes and enhance transfection efficiency.[8] However, it has been reported that PEI induced strong cytotoxicity.[9] The toxicity of a pDNA/PEI complex was about seven times higher than that of a pDNA/chitosan complex.[10] Therefore, in this study, we prepared pDNA/chitosan/sugar–PEG-A/C ternary complexes and evaluated their transfection efficiency in vitro.

Chitosan was obtained from Yaizu Suisankagaku Industry (Shizuoka, Japan). The average molecular weight was 40000, and the degree of deacetylation was 85%. PEG-A/C and sugar–PEG-A/Cs were synthesized according to a previous paper.[8] The substitution degrees of maltose and lactose were 2.9 and 4.4 per molecule, respectively (Figure 1). The molecular weight of Mal–PEG-A/C was 9770, and that of Lac–PEG-A/C was

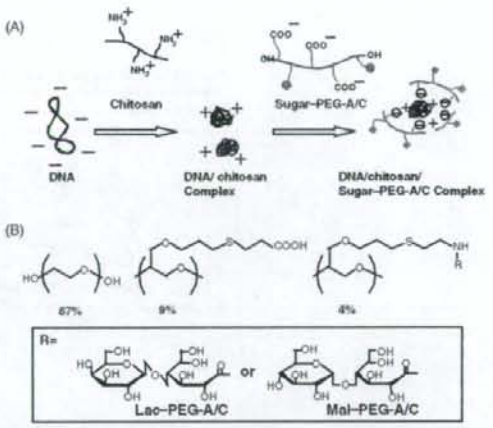

Figure 1. (A) A scheme for the formation of pDNA/chitosan/sugar–PEG-A/C ternary complexes. (B) Structure of sugar–PEG-A/Cs.

10300. A pDNA/chitosan complex was prepared according to the method previously reported.[3] The P/N ratio, which is the ratio of phosphate anion (P) of pDNA to the amino group (N) of chitosan, was 1/5. Ternary complexes were prepared by mixing preformed pDNA/chitosan complexes with aqueous solutions of PEG-A/C or sugar–PEG-A/Cs at appropriate P/N/C (C is carboxyl group of PEG-A/C) ratios for 15 min. In this study, pGL3-Luc (Promega) encoding the *luciferase* gene was employed as pDNA.

AFM observation with SPM-300 (Seiko Instruments Inc., Japan) indicated that the pDNA/chitosan complexes ($P/N > 3$) showed spherical structures of 200 nm in diameter. The morphology and size of the pDNA/chitosan/PEG-A/C complex at $P/N/C = 1/5/20$ were similar to the pDNA/chitosan complex. The particle size of the pDNA/chitosan/sugar–PEG-A/C complex was about 500 nm at $N/P/C = 1/5/10$ and $1/5/20$. There was no obvious morphological difference between the pDNA/chitosan/Mal–PEG-A/C and pDNA/chitosan/Lac–PEG-A/C complexes.

The zeta potential was determined at various P/N/C ratios of the ternary complexes with a ZeeCom (Microtec Co., Ltd., Japan) at 25 °C (Figure 2). The zeta potential of the pDNA/chitosan complex at $P/N = 1/5$ was +49 mV, and was decreased by coating it with sugar–PEG-A/Cs. The zeta potentials of the pDNA/chitosan/sugar–PEG-A/C complexes were negative at $P/N/C = 1/5/10$ and $1/5/20$. Therefore, it is considered that the surface of the cationic pDNA/chitosan complex was coated with anionic Mal–PEG-A/C and Lac–PEG-A/C.

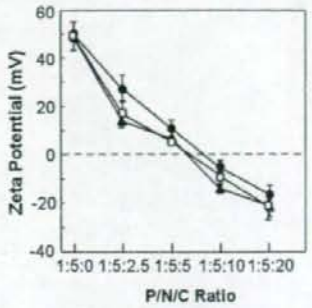

Figure 2. Zeta potentials of pDNA/chitosan/PEG-A/C (closed triangle), pDNA/chitosan/Mal–PEG-A/C (open square), and pDNA/chitosan/Lac–PEG-A/C (closed circle) complexes in 20 mM HEPES buffer. [pDNA] = 1.5 μg/mL.

The resistance of ternary complexes to degradation by DNaseI was investigated by agarose gel electrophoresis. The naked pDNA was completely digested by DNaseI (0.1 U) 50 mM Tris-HCl buffer containing 10 mM $MgCl_2$ and 100 mM NaCl at 37 °C for 30 min. On the other hand, the pDNA/chitosan and pDNA/chitosan/sugar–PEG-A/C complexes showed markedly improved resistance against DNaseI.

Luciferase activities of pDNA/chitosan/PEG-A/C complexes were investigated for B16 mouse melanoma cells. The transfection efficiency of the pDNA/chitosan/PEG-A/C complex at P/N/C = 1/5/2.5 decreased to one tenth that of the pDNA/chitosan complex. The transfection efficiencies of the ternary complexes were recovered by increasing the amount of PEG-A/C, and that of the complex of P/N/C = 1/5/40 was almost comparable with that of the pDNA/chitosan complex.

Next, the transfection efficiencies of the pDNA/chitosan/sugar–PEG-A/C complexes were investigated for B16 cells (Figure 3). The transfection efficiencies of pDNA/chitosan/

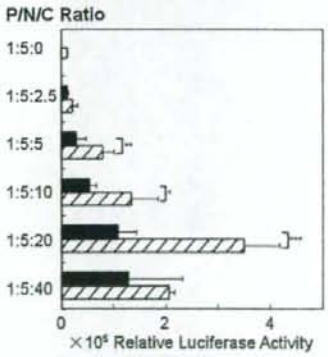

Figure 3. Transfection efficiencies of pDNA/chitosan/Lac–PEG-A/C (black bar) and pDNA/chitosan/Mal–PEG-A/C (cross-hatched bar) complexes at different P/N/C ratios. The luciferase activity of naked pDNA was normalized to 100. The luciferase activity of B16 cells transfected with 2.5 μg of pDNA per 2×10^5 cells represents the mean values of three experiments. The transfection time was 4 h, and post-transfection time was 20 h. * $P < 0.1$, ** $P < 0.05$, *** $P < 0.01$.

Lac–PEG-A/C and pDNA/chitosan/Mal–PEG-A/C complexes at P/N/C = 1/5/20 were 5.5- and 20-fold higher, respectively, than that of the pDNA/chitosan complex. The increased transfection efficiencies of the pDNA/chitosan/sugar–PEG-A/C complexes were also observed for human hepatoma HepG2 cells.

Since both the pDNA/chitosan/Lac–PEG-A/C and pDNA/chitosan/Mal–PEG-A/C complexes showed enhanced transfection efficiencies compared with pDNA/chitosan complexes, it was considered that physicochemical stability contributed to their high transfection efficiency. Thus, the interactions of the DNA complexes with anionic serum albumin and glycosaminoglycan (chondroitin sulfate) were investigated. The turbidity (at 350 nm) of the pDNA/chitosan complex markedly increased depending on the concentration of BSA (0.1–1 mg/mL), whereas those of the pDNA/chitosan/Mal–PEG-A/C complexes were significantly suppressed. Furthermore, the release of pDNA from the pDNA/chitosan and pDNA/chitosan/Mal–PEG-A/C complexes in the presence of 2% chondroitin sulfate was investigated by agarose gel electrophoresis. Though pDNA was released from the pDNA/chitosan complex, no release was observed from the pDNA/chitosan/Mal–PEG-A/C complex. These results suggested that the stability of the pDNA/chitosan complex against polyanions was improved by coating its surface with sugar–PEG-A/Cs. Improvement of the physicochemical stability of chitosan-containing gene carriers would be preferable for in vivo administration.

This work was partly supported by the Special Coordination of Funds for Promoting Science and Technology from the Ministry of Education, Culture, Sports, Science and Technology, Japan (T. S.).

References and Notes

1 S. Hirano, H. Seino, Y. Akiyama, I. Nonaka, *Polym. Eng. Sci.* **1988**, *59*, 897.
2 T. Sato, N. Shirakawa, H. Nishi, Y. Okahata, *Chem. Lett.* **1996**, 725.
3 a) T. Ishii, Y. Okahata, T. Sato, *Biochim. Biophys. Acta* **2001**, *1514*, 51. b) T. Sato, T. Ishii, Y. Okahata, *Biomaterials* **2001**, *22*, 2075.
4 a) K. Roy, H.-Q. Mao, S.-K. Huang, K. W. Leong, *Nature Med.* **1999**, *5*, 387. b) L. Illum, I. Jabbal-Gill, M. Hinchcliffe, A. N. Fisher, S. S. Davis, *Adv. Drug Delivery Rev.* **2001**, *51*, 81.
5 a) M. Hashimoto, M. Morimoto, H. Saimoto, Y. Shigemasa, T. Sato, *Bioconjugate Chem.* **2006**, *17*, 309. b) M. Hashimoto, M. Morimoto, H. Saimoto, Y. Shigemasa, H. Yanagie, M. Eriguchi, T. Sato, *Biotech. Lett.* **2006**, *28*, 815.
6 M. Ogris, S. Brunner, S. Schüller, R. Kircheis, E. Wagner, *Gene Ther.* **1999**, *6*, 595.
7 a) H.-Q. Mao, K. Roy, V. L. Troung-Le, K. A. Janes, K. Y. Lin, Y. Wang, J. T. August, K. W. Leong, *J. Controlled Release* **2001**, *70*, 399. b) I. K. Park, T. H. Kim, Y. H. Park, B. A. Shin, E. S. Choi, E. H. Chowdhury, T. Akaike, C. S. Cho, *J. Controlled Release* **2001**, *76*, 349.
8 Y. Koyama, E. Yamada, T. Ito, Y. Miautani, T. Yamaoka, *Macromol. Biosci.* **2002**, *2*, 251.
9 S. M. Moghimi, P. Symonds, J. C. Murray, A. C. Hunter, G. Debska, A. Szewczyk, *Mol. Ther.* **2005**, *11*, 990.
10 M. Köping-Höggård, I. Tubulekas, H. Guan, K. Edwards, M. Nilsson, K. M. Vårum, P. Artursson, *Gene Ther.* **2001**, *8*, 1108.
11 Supporting Information is available electronically on the CSJ-Journal Web site, http://www.csj.jp/journals/chem-lett.

Published on the web (Advance View) February 2, 2008; doi:10.1246/cl.2008.266

Available online at www.sciencedirect.com
ScienceDirect
Carbohydrate Research 343 (2008) 831–838
Carbohydrate RESEARCH

Glycosylation of dodecyl 2-acetamido-2-deoxy-β-D-glucopyranoside and dodecyl β-D-galactopyranosyl-(1→4)-2-acetamido-2-deoxy-β-D-glucopyranoside as saccharide primers in cells

Toshinori Sato,[a,*] Minako Takashiba,[a] Rumi Hayashi,[a] Xingyu Zhu[a] and Tatsuya Yamagata[b]

[a]*Department of Biosciences and Informatics, Keio University, Yokohama 223-8522, Japan*
[b]*Shenyang Pharmaceutical University, PO Box 29, School of Pharmaceutical Engineering, Shenyang 110016, PR China*

Received 3 July 2007; received in revised form 26 December 2007; accepted 16 January 2008
Available online 26 January 2008

Abstract—Syntheses of oligosaccharides expressed on cells are indispensable for the improvement of the functional analyses of the oligosaccharides and their applications. We are developing saccharide primers for synthesizing oligosaccharides using living cells. In this study, dodecyl 2-acetamido-2-deoxy-β-D-glucopyranoside (GlcNAc-C12) and dodecyl β-D-galactopyranosyl-(1→4)-2-acetamido-2-deoxy-β-D-glucopyranoside (LacNAc-C12) were examined for their abilities to prime the syntheses of neolacto-series oligosaccharides in HL60 cells. When GlcNAc-C12 was incubated with HL60 cells in serum-free medium for 2 days, 14 kinds of glycosylated products were collected from the culture medium. They were separated by high-performance liquid chromatography. The sequences of the products were determined to be neolacto-series oligosaccharides including Lewis^X, sialyl Lewis^X, polylactosamine, and sialylpolylactosamine by mass spectrometry. GlcNAc-C12 was also glycosylated by B16 cells and gave sialyllactosamine. Furthermore, LacNAc-C12 gave similar glycosylated products to GlcNAc-C12.

Keywords: Saccharide primer; *N*-Acetylglucosamine; *N*-Acetyllactosamine; Oligosaccharide; Glycosylation; Animal cells

1. Introduction

The importance of technology to synthesize oligosaccharides expressed on mammalian cells has been indicated by the elucidation of their roles in cell function. We have been developing saccharide primer methods to synthesize oligosaccharides using the glycan biosynthesis system in cells. A saccharide primer is a glycolipid analogue to be glycosylated by cells in culture. Yamagata and co-workers have developed amphiphilic glycolipid analogues such as alkyllactosides.[1,2] Dodecyl β-lactoside (Lac-C12) as a saccharide primer was incorporated into B16 melanoma cells and was glycosylated by glycosyltransferase. The glycosylated product was secreted from the cells. Structural analyses indicated that the product was sialyllactose, which is the carbohydrate portion of GM3 normally expressed on the surface of mouse B16 melanoma cells.

Other primers as substrates for glycosyltransferase in cells have been described in several reports. β-D-Xylosides have been developed as an initiator of glycosaminoglycan biosynthesis.[3,4] Acetylated Xylβ1-6Gal-*O*-2-naphthol and acetylated Galβ1-4GlcNAcβ-*O*-naphthalenemethanol (NM) were investigated as inhibitors of the glycosyltransferase in cells.[5] Furthermore, acetylated Galβ1-4GlcNAcβ-NM and acetylated GlcNAcβ1-3Galβ-NM inhibited the biosynthesis of endogenous sialyl Lewis^X, and they were also glycosylated in human promyelocytic leukemia HL60 cells.[6]

The glycosylation of the saccharide primers was suggested to be dependent on the cell lines, because different types of cells have different intrinsic glycan biosynthesis

* Corresponding author. Tel.: +81 45 566 1771; fax: +81 45 566 1447; e-mail: sato@bio.keio.ac.jp

0008-6215/$ - see front matter © 2008 Elsevier Ltd. All rights reserved.
doi:10.1016/j.carres.2008.01.022

systems. Therefore, a saccharide library could be synthesized by combining various saccharide primers and cells. HL60 cells are known to express ganglioside GM3 and neolacto-series oligosaccharides. When Lac-C12 was incubated with HL60 cells, only the sialylated product (sialyllactose) was obtained, but not neolacto-series oligosaccharides. Therefore, in the present study, we synthesized dodecyl 2-acetamido-2-deoxy-β-D-glucopyranoside (GlcNAc-C12) and dodecyl β-D-galactopyranosyl-(1→4)-2-acetamido-2-deoxy-β-D-glucopyranoside (LacNAc-C12) as saccharide primers (Fig. 1), and the glycosylation reactions of those primers by HL 60 cells and B16 cells were examined.

2. Results

2.1. Glycosylation of GlcNAc-C12 by HL60 cells

HL60 cells were employed to examine the usefulness of GlcNAc-C12 as saccharide primer for the synthesis of neolacto-series oligosaccharides. After incubation of 50 μM of GlcNAc-C12 with HL60 cells, glycosylated products and unreacted primers were collected from the culture medium and cell fraction using a Sep-Pak C_{18} column. The glycosylated products adsorbed to the column were eluted using mixed solvents of methanol and water. The glycosylated products were largely detected from the culture medium. The acidic and neutral products were eluted with 3:7 MeOH–H_2O, and 1:9 MeOH–H_2O, respectively. As shown in Figure 2A, HPTLC (high-performance thin-layer chromatography) indicated that the fractions eluted with 3:7 MeOH–H_2O contained four neutral products (N1–N4), and the fractions eluted with 1:9 MeOH–H_2O contained six acidic products (A1–A6). Next, the neutral and acidic products were separated by high-performance liquid chromatography (HPLC). The four neutral products were separated using 70:28:2 $CHCl_3$–MeOH–H_2O as shown in Figure 2B. N1, N2, N3, and N4 were detected in fraction numbers 7–9, 11–12, 35–40, and 70–80, respectively. The four acidic products (A1–A4) were separated using 70:28:2 $CHCl_3$–MeOH–H_2O as shown in Figure 2C. A1, A2, A3, and A4 were detected in fraction numbers 17–19, 20–23, 26–28, and 45–50, respectively. Two acidic products (A5–A6) were separated using 60:35:5 $CHCl_3$–MeOH–H_2O as shown in Figure 2D. A4 and A5 were detected in fraction numbers 10 and 11–13, respectively.

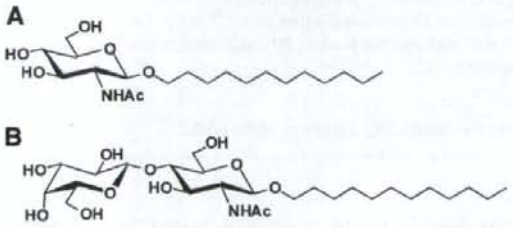

Figure 1. Saccharide primers, GlcNAc-C12 (A) and LacNAc-C12 (B), employed in this study.

2.2. Analyses of the chemical structures of products by mass spectrometry

Analyses of the structures of products separated by HPLC were carried out by MALDI-TOFMS (matrix-assisted laser desorption and ionization time-of-flight mass spectrometry). The observed masses and the deduced sequences of the glycosylated products are shown in Table 1. The mobility of N1 on HPTLC was same as that of synthetic Galβ1-4GlcNAc-C12 (LacNAc-C12), and the non-reducing hexose of N1 was cleaved by jack bean β-galactosidase (data not shown). Furthermore, the positive MALDI-PSD (post-source decay)

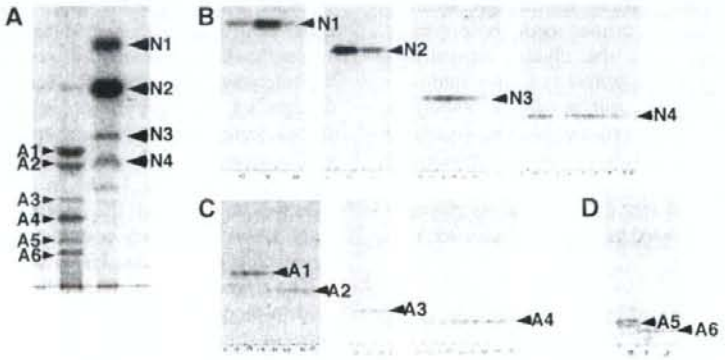

Figure 2. HPTLC of the products collected using a Sep-Pak C_{18} column (A), and purified by HPLC (B, C, and D) for the glycosylation of GlcNAc-C12 by HL60 cells.

Table 1. Deduced sequences and mass observed by MALDI-TOF-MS for the glycosylated products from GlcNAc-C12

Product	Sequence	Observed mass
N1	Galβ1-4GlcNAc-C12	574.1 $[M+Na]^+$
N2	Galβ1-4(Fucα1-3)-GlcNAc-C12	720.1 $[M+Na]^+$
N3	Galβ1-4GlcNAcβ1-3Galβ1-4GlcNAc-C12	939.1 $[M+Na]^+$
N4	Galβ1-4GlcNAcβ1-3Galβ1-4(Fucα1-3)GlcNAc-C12	1085.3 $[M+Na]^+$
A1	NeuNAcα2-3Galβ1-4GlcNAc-C12	841.4 $[M-H]^-$
A2	NeuNAcα2-6Galβ1-4GlcNAc-C12	841.4 $[M-H]^-$
A3	NeuNAc-(Galβ1-4GlcNAc)$_2$-C12	1230.1 $[M-H]^-$
A4	Fucose+A3	1376.3 $[M-H]^-$
A5	NeuNAc-(Galβ1-4GlcNAc)$_3$-C12	1595.9 $[M-H]^-$
A6	Fucose+A5	1742.0 $[M-H]^-$

spectrum (Table 2) revealed a peak at m/z 305.32 corresponding to $^{0,2}A_2$ fragment ($+Na^+$, intramolecular cleavage of GlcNAc). The results of MALDI-PSD agreed with the values in the literature.[7] Thus, N1 was determined to be Galβ1-4GlcNAc-C12. N2 was predicted to be H antigen (Fuc-Gal-GlcNAc-C12) or Lewis^X (Gal-(Fuc)-GlcNAc-C12) from the peak of m/z 720.1 ($[M+Na]^+$) of the MALDI-TOF-MS spectrum (Table 1). The MALDI-PSD spectrum of N2 (Table 2) revealed peaks at m/z 558.4 corresponding to $Y_{1\beta}$ (Fuc-GlcNAc-C12+Na^+) and m/z 305.4 corresponding to the $Y_{1\alpha}/^{0,2}A_2$ fragment ($+Na^+$). The observed fragment ions of N2 were similar to the MALDI-PSD spectrum of Lewis^X reported in the literature.[7] Therefore, N2 was determined to be Lewis^X. N3 was predicted to be Gal-GlcNAc-Gal-GlcNAc-C12 from the peak of m/z 939.1 ($[M+Na]^+$) of the MALDI-TOF-MS spectrum (Table 1). The MALDI-PSD spectrum of N3 (Table 2) revealed peaks at m/z 670.5 corresponding to $^{0,2}A_4$ fragment ($+Na^+$) and m/z 305.3 corresponding to $^{0,2}A_2$ fragment ($+Na^+$), suggesting the existence of two β-(1→4) lactosamine units. N4 was predicted to be fucosylated N3 from the peak of m/z 1085.3 ($[M+Na]^+$) of the MALDI-TOF-MS spectrum (Table 1). The MALDI-PSD spectrum of N4 (Table 2) revealed a peak at m/z 558.6 corresponding to $Y_{1\beta}$ (Fuc-GlcNAc-C12+Na^+), and fragmentation ions were similar to those of N3, suggesting that N4 is Galβ1-4GlcNAcβ1-3Galβ1-4(Fucα1-3)GlcNAc-C12. HL60 cells express FUT4, which transfers fucose to lactosamine.[8] Furthermore, it has been reported that FUT4 preferentially transfers fucose to inner GlcNAc residues.[9] The structure of N5 agreed with that of the endogenous glycan reported in the literature.[8,9]

Though the mobilities of A1 and A2 on HPTLC were different, the MALDI-TOF-MS spectra of them revealed the same mass of 841.4 ($[M-H]^-$), corresponding to NeuNAc-Gal-GlcNAc-C12 (sLacNAc-C12, Table 1). Since A1 and A2 are considered to have different linkages of *N*-acetylneuraminic acid to galactose, the

Table 2. Fragment ions observed by MALDI-PSD spectrum for the glycosylated products from GlcNAc-C12

Product	Fragments
N1	226.4 ($[Y_1/B_2+Na]^+$), 305.3 ($[^{0,2}A_2+Na]^+$), 388.4 ($[B_2+Na]^+$), 412.4 ($[Y_1+Na]^+$),
N2	226.3 ($[Y_{1\alpha}/Y_{1\beta}/B_2+Na]^+$), 305.4 ($[Y_{1\alpha}/^{0,2}A_2+Na]^+$), 370.5 ($[Z_1/B_2+Na]^+$), 388.3 ($[Y_{1\alpha}/B_2+Na]^+$), 412.4 ($[Y_{1\alpha}/Y_{1\beta}+Na]^+$), 534.4 ($[B_2+Na]^+$), 556.4 ($[Z_1+Na]^+$), 558.4 ($[Y_{1\beta}+Na]^+$), 574.6 ($[Y_{1\alpha}+Na]^+$)
N3	226.3 ($[Y_3/B_2+Na]^+$, $[B_4/Y_1+Na]^+$), 305.3 ($[^{0,2}A_2+Na]^+$), 388.2 ($[B_2+Na]^+$ or $[B_4/Y_2+Na]^+$), 406.4 ($[C_2+Na]^+$), 412.5 ($[Y_1+Na]^+$), 550.3 ($[B_3+Na]^+$), 574.5 ($[Y_2+Na]^+$), 670.5 ($[^{0,2}A_4+Na]^+$), 753.7 ($[B_4+Na]^+$), 777.9 ($[Y_3+Na]^+$)
N4	226.4 ($[Y_3/B_2+Na]^+$, $[Y_{1\alpha}/B_4/Y_{1\beta}+Na]^+$), 305.3 ($[^{0,2}A_2+Na]^+$), 388.5 ($[B_2+Na]^+$ or $[Y_{1\alpha}/B_4/Y_2+Na]^+$), 406.5 ($[C_2+Na]^+$), 412.7 ($[Y_{1\alpha}/Y_{1\beta}+Na]^+$), 550.6 ($[B_3+Na]^+$), 558.7 ($[Y_{1\beta}+Na]^+$), 574.9 ($[Y_{1\alpha}/Y_2+Na]^+$), 670.4 ($[Y_{1\alpha}/^{0,2}A_4+Na]^+$), 720.6 ($[Y_2+Na]^+$), 778.0 ($[Y_{1\alpha}/Y_3+Na]^+$), 901.9 ($[Y_3+Na]^+$), 940.0 ($[Y_{1\alpha}+Na]^+$)
A3	388.3 ($[Y_4/B_3+Na]^+$, $[Y_2/B_5+Na]^+$), 406.5 ($[Y_4/C_3+Na]^+$), 412.4 ($[Y_1+Na]^+$), 476.3 ($[B_2+Na]^+$), 550.5 ($[Y_4/B_4+Na]^+$), 574.6 ($[Y_2+Na]^+$), 634.9 ($[^{0,2}A_3+Na+K-H]^+$), 679.6 ($[B_3+Na]^+$), 753.8 ($[B_5/Y_3+Na]^+$), 777.7 ($[Y_3+Na]^+$), 939.8 ($[Y_4+Na]^+$)
A4	336.4 ($[B_1+2Na-H]^+$), 388.4 ($[Y_4/B_3+Na]^+$ or $[Y_{1\alpha}/Y_2/B_5+Na]^+$), 406.5 ($[Y_4/C_3+Na]^+$), 412.3 ($[Y_{1\alpha}/Y_{1\beta}+Na]^+$), 476.5 ($[B_2+Na]^+$), 550.6 ($[Y_4/B_4+Na]^+$), 558.9 ($[Y_{1\beta}+Na]^+$), 574.6 ($[Y_{1\alpha}/Y_2+Na]^+$), 634.9 ($[^{0,2}A_3+Na+K-H]^+$), 679.6 ($[B_3+Na]^+$), 720.9 ($[Y_2+Na]^+$), 777.8 ($[Y_{1\alpha}/Y_3+Na]^+$), 841.3 ($[B_4+Na]^+$), 923.9 ($[Y_3+Na]^+$), 939.6 ($[Y_{1\alpha}/Y_4+Na]^+$), 1085.4 ($[Y_4+Na]^+$), 1230.8 ($Y_{1\alpha}$)
A5	388.1 ($[Y_6/B_3+Na]^+$, $[B_5/Y_4+Na]^+$ or $[B_7/Y_2+Na]^+$), 406.2 ($[Y_6/C_3+Na]^+$ or $[C_5/Y_4+Na]^+$), 550.3 ($[B_6/Y_4+Na]^+$), 574.6 ($[Y_2+Na]^+$), 591.2 ($[Y_5/B_5+Na]^+$ or $[B_7/Y_4+Na]^+$), 596.7 ($[^{0,2}A_3+Na]^+$), 634.9 ($[^{0,2}A_3+Na+K-H]^+$), 670.2 ($[Y_6/^{0,2}A_5+Na]^+$, $[Y_4/^{0,2}A_7+Na]^+$), 679.5 ($[B_3+Na]^+$), 753.6 ($[Y_6/B_5+Na]^+$ or $[B_7/Y_4+Na]^+$, 777.6 ($[Y_3+Na]^+$), 916.8 ($[Y_4+H]^+$), 939.5 ($[Y_4+Na]^+$), 999.8 ($[^{0,2}A_5+Na]^+$), 1045.1 ($[B_5+Na]^+$), 1142.7 ($[Y_5+Na]^+$), 1305.0 ($[Y_6+Na]^+$)
A6	388.6 ($[Y_6/B_3+Na]^+$, $[B_5/Y_4+Na]^+$ or $[Y_{1\alpha}/B_7/Y_2+Na]^+$), 406.8 ($[Y_6/C_3+Na]^+$, $[C_5/Y_4+Na]^+$), 550.5 ($[B_6/Y_4+Na]^+$), 574.9 ($[Y_{1\alpha}/Y_2+Na]^+$), 591.3 ($[Y_5/B_5+Na]^+$ or $[Y_{1\alpha}/B_7/Y_3+Na]^+$), 596.2 ($[^{0,2}A_3+Na]^+$), 634.4 ($[^{0,2}A_3+Na+K+H]^+$), 720.2 ($[Y_2+Na]^+$), 753.8 ($[Y_{1\alpha}/Y_6/^{0,2}A_5+Na]^+$ or $[Y_{1\alpha}/Y_4/^{0,2}A_7+Na]^+$), 777.6 ($[Y_{1\alpha}/Y_3+Na]^+$), 899.9 ($[Y_4/B_7+Na]^+$), 916.9 ($[Y_{1\alpha}/Y_4+H]^+$), 923.9 ($[Y_3+Na]^+$), 939.8 ($[Y_{1\alpha}/Y_3+Na]^+$), 1000.0 ($[Y_{1\alpha}/^{0,2}A_5+Na]^+$), 1045.5 ($[B_5+Na]^+$), 1085.7 ($[Y_4+Na]^+$), 1288.8 ($[Y_5+Na]^+$), 1304.5 ($[Y_{1\alpha}/Y_6+Na]^+$), 1451.0 ($[Y_6+Na]^+$), 1472.6 ($[Y_6+2Na-H]^+$), 1596.1 ($[Y_{1\alpha}+Na]^+$)

enzymatic cleavages of sLacNAc-C12 by neuraminidases were examined. The neuraminidases employed in this study were *Arthrobacter ureafacience* neuraminidase, which hydrolyzes α-(2→3), α-(2→6), and α-(2→8) linkages,[10] and *Macrobdella decora* neuraminidase, which hydrolyzes α-(2→3) linkage.[11] Though *N*-acetylneuraminic acid of A1 was cleaved by both neuraminidases, that of A2 was cleaved by the *A. ureafacience* neuraminidase but not by the *M. decora* neuraminidase. The hydrolyzed products showed the same mobility as synthetic Galβ1-4GlcNAc-C12. Next, ESI (electrospray ionization)-CID (collision-induced dissociation) was employed to distinguish between A1 and A2. The ESI-CID spectra of A1 and A2 showed peaks of *m/z* 887.5 ($[M+2Na-H]^+$) corresponding to NeuNAc-Gal-GlcNAc-C12, and *m/z* 574.3 ($[(M\text{-anNeuNAc})+Na]^+$) corresponding to Y_2 fragment (Gal-GlcNAc-C12). The relative intensity of Y_2 (*m/z* 574.3) to the parent peak (*m/z* 887.5) showed significant differences between A1 and A2, and was 0.68 for A1 and 0.03 for A2. It has been reported that α-(2→3) sialyl linkage was distinguished from α-(2→6) sialyl linkage based on the ESI-CID spectra.[12] In the literature, the fragmentation ions produced by the cleavage of the α-(2→3) sialyl linkage showed much higher intensity than those produced by the cleavage of the α-(2→6) sialyl linkage. Therefore, from the results of enzymatic digestions and ESI-CID spectra, A1 and A2 were determined to be NeuNAcα2-3Galβ1-4GalNAc-C12 and NeuNAcα2-6Galβ1-4GalNAc-C12, respectively.

The MALDI-TOFMS spectra of A3 and A5 (Table 1) revealed peaks of *m/z* 1230.1 ($[M-H]^-$) corresponding to NeuNAc-(Gal-GlcNAc)$_2$-C12 and *m/z* 1571.7 ($[M-H]^-$) corresponding to NeuNAc-(Gal-GlcNAc)$_3$-C12. A3 was considered to be produced by the sialylation of N4. The MALDI-TOF-MS spectra of A4 and A6 revealed peaks of *m/z* 1352.7 ($[M-H]^-$) corresponding to fucosylated A3 and *m/z* 1779.0 ($[M-H]^-$) corresponding to fucosylated A5. The positive-ion mode MALDI-PSD spectrum of A4 (Table 2) revealed peaks at *m/z* 558.9 corresponding to $Y_{1\beta}$ (Fuc-GlcNAc-C12+Na^+) and *m/z* 720.9 corresponding to Y_2 (Fuc+Gal-GlcNAc-C12+Na^+). The positive-ion mode MALDI-PSD spectrum of A6 (Table 2) also revealed a peak at *m/z* 720.2 corresponding to Y_2 (Fuc+Gal-GlcNAc-C12+Na^+), *m/z* 923.9 corresponding to Y_3 (Fuc+Gal-GlcNAc-Gal-GlcNAc-C12+Na^+), and *m/z* 1085.7 corresponding to Y_4 (Fuc+Gal-GlcNAc-Gal-GlcNAc-C12+Na^+). These MALDI-PSD spectra suggested that the fucose moieties in A4 and A6 were linked to the innermost GlcNAc residue. It has been reported that HL60 cells express α-(1→3)-fucosyltransferase, and fucosylated monosialyl glycolipids having similar structures to A4 and A6 were detected in HL60 cells.[13] Though the linkages of *N*-acetylneuraminic acid in A3, A4, A5, and A6 could not be determined in the present study, they were inferred to be α-(2→3) from the structural analysis of the sialyl linkage of sialylpolylactosamine expressed in HL60 cells.[14]

2.3. Glycosylation of LacNAc-C12 by HL60 cells

Next, the glycosylation of LacNAc-C12 by HL60 cells was examined. After incubation of HL60 cells with 50 μM LacNAc-C12 for 2 days, glycosylated products and unreacted primer were isolated from the culture medium. The glycosylated products collected using a Sep-Pak C_{18} column were analyzed by HPTLC. One neutral product and six acidic products were detected. The analyses of mobility on HPTLC and the mass spectrum indicated that the products glycosylated from LacNAc-C12 were the same as those from GlcNAc-C12. The neutral product was N2 and the acidic products were A1–A6.

2.4. Comparison of GlcNAc-C12 and LacNAc-C12 as glycosyl acceptors in B16 cells

After incubation of 50 μM GlcNAc-C12 or LacNAc-C12 with B16 cells for 2 days, glycosylated products were isolated from the culture medium. The glycosylated products were analyzed by HPTLC and MALDT-TOF-MS. Using GlcNAc-C12, two glycosylated products were detected. One was Gal-GlcNAc-C12, whose mobility on HPTLC was the same as that of synthetic LacNAc-C12. The other was considered to be NeuNAc-Gal-GlcNAc-C12 (sLacNAc-C12) from the mass spectrum. For LacNAc-C12, the detected product was also suggested to be sLacNAc-C12 from the mobility on HPTLC and from the mass spectrum. To determine the linkage of the sialic acid, the product was treated with neuraminidases from *A. ureafaciens* and *M. decora*. Since the glycosylated product sLacNAc-C12 was hydrolyzed by both sialidases, the linkage of NeuNAc-Gal was determined to be α-(2→3). The amount of sLacNAc-C12 derived from GlcNAc-C12 was two times higher than that from LacNAc-C12, when the dose of saccharide primers was 50 μM (Fig. 3). The glycosylation efficiency of GlcNAc-C12 in cells was higher than that of LacNAc-C12 in cells. When the dose of GlcNAc-C12 was 50 μM (250 nmol), the amount of sLacNAc-C12 was determined to be 7.5 nmol by quantitative analysis using GM1 as standard.

2.5. Cell growth in the presence of saccharide primers

B16 cells were cultured in the absence and the presence of 50 μM GlcNAc-C12 and LacNAc-C12 for 2 days. The cell growth in the presence of the saccharide primers was almost similar to that of control (Fig. 4). Cell growth of HL60 cells was also investigated in the presence of 50 μM GlcNAc-C12 for 2 days (data not

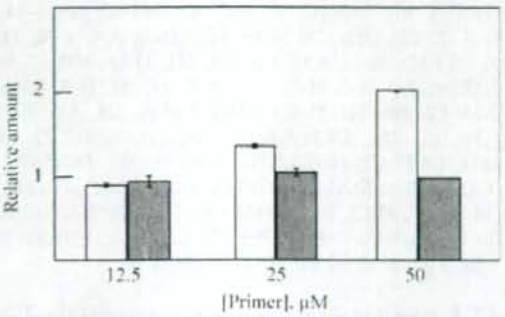

Figure 3. Relative amounts of NeuNAc-Gal-GlcNAc-C12 glycosylated from GlcNAc-C12 (white column) and Gal-GlcNAc-C12 (black column) by B16 melanoma cells (2×10^6 cells). The relative amounts were analyzed by densitometry at 540 nm followed by staining with resorcinol–HCl. The dose of saccharide primers was 50 μM.

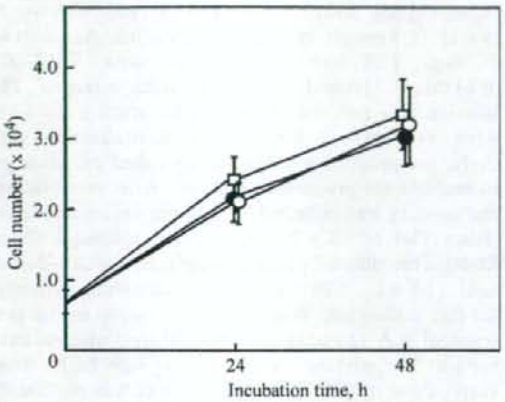

Figure 4. Growth of B16 cells cultured in the absence (closed circle) and the presence of 50 μM GlcNAc-C12 (open circle) and LacNAc-C12 (open square).

shown). The primers showed no cytotoxicity at the present experimental conditions.

3. Discussion

Convenient synthesis of glycan structures present on cells is important for the study to elucidate glycan function. Since saccharide primers can act as substrates for glycosyltransferases present in cells, they are useful for the synthesis of oligosaccharides expressed in cells. Saccharide primers are building blocks for constructing an oligosaccharide library by biocombinatorial synthesis that is combination of different saccharide primers and a variety of cells. It has been reported that Lac-C12, which is a mimicry of lactosylceramide, was useful to synthesize the oligosaccharides of glycosphingolipids (GSL). For example, Lac-C12 gave GM3 oligosaccharide when incubated with B16 melanoma cells. Furthermore, 12-azido dodecyl-β-lactoside (Lac-C12-N3) was synthesized with the aim of preparing glycan arrays or glycopolymers. Lac-C12-N3 was also glycosylated by cells as well as Lac-C12[15] and could be conjugated to solid supports by the modified Staudinger reaction or condensation reaction followed by reduction to the amino group for detecting carbohydrate recognition.[16]

For the construction of oligosaccharide libraries, it is important to synthesize various oligosaccharides. In our ongoing studies, it has been found that Lac-C12 gave rise to various oligosaccharides of ganglio- and globo-series gangliosides. Then, in the present study, we synthesized novel saccharide primers to selectively obtain neolacto-series oligosaccharides. In the biosynthesis of neolacto-series glycans, the lactosamine unit of Galβ1-4GlcNAc is the precursor region for sugar elongation. Thus, saccharide primers containing GlcNAc and LacNAc would be substrates for glycosyltransferases synthesizing neolacto-series oligosaccharides. In the literature, Esko and co-workers have reported that disaccharide primers such as peracetylated Galβ1-4GlcNAc-NM were fucosylated to Galβ1-4(Fucα1-3)GlcNAc-NM, and peracetylated GlcNAcβ1-3Gal-NM was converted to Galβ1-4(Fucα1-3)GlcNAcβ1-3Gal-NM, NeuNAcα2-3Galβ1-4GlcNAcβ1-3Gal-NM, and NeuNAcα2-3Galβ1-4(Fucα1-3)GlcNAcβ1-3Gal-NM by U937 human histiocytic lymphoma cells.[6] Those peracetylated primers were glycosylated after deacetylation in cells. In our study, deacetylated saccharide primer was used for the synthesis of oligosaccharides by cells. GlcNAc-C12 and LacNAc-C12 gave Le^X, sLe^X, polylactosamine, sialylated polylactosamine, and sialylated/fucosylated polylactosamine by incubating with HL60 cells. These oligosaccharides were similar to endogenous glycans observed in HL60.[17] The complex glycosylated products were clearly separated by HPLC, and their chemical structures were determined by enzymatic digestion and mass spectrometry. Separation and structural elucidation of the products were very convenient compared to the endogenous GSLs because the saccharide primers had a uniform aglycon structure.

Since GlcNAc-C12 gave similar glycosylated products to LacNAc-C12, we could conclude that monosaccharide primers as well as disaccharide primers are useful for the synthesis of oligosaccharides. It has been reported that the glycosylation efficiencies of saccharide primers were dependent on their hydrophilic–hydrophobic balance.[2,18] More hydrophilic saccharide primers cannot be internalized into cells, while more hydrophobic ones are strongly adsorbed to the cell membrane. Although the glycosylation efficiency of GlcNAc-C12 was higher than that of LacNAc-C12 in the present study, the structure for giving optimum glycosylation

efficiency would be determined by varying the hydrocarbon chain length.

In conclusion, saccharide primers such as GlcNAc-C12 and LacNAc-C12 were developed to synthesize neolacto-series oligosaccharides using mammalian cells. The glycosylated products were separated by HPLC, and the sequences were determined by enzymatic digestion and mass spectrometry. The saccharide primers employed in this study are expected to be useful for synthesizing oligosaccharides expressed in mammalian cells.

4. Experimental

4.1. Synthesis of dodecyl 2-acetamido-2-deoxy-β-D-glucopyranoside (GlcNAc-C12)

2-Acetamido-1,3,4,6-tetra-*O*-acetyl-2-deoxy-D-glucopyranoside (Ac_4-GlcNAc) was prepared by reacting *N*-acetylglucosamine (2.5 g, 11.3 nmol, GlcNAc, Sigma) with Ac_2O (15 mL, 159 mmol, Wako Pure Chemicals) in 30 mL of pyridine according to the literature.[19] Ac_4-GlcNAc (3 g, 7.71 mmol) was mixed with TMS-OTf (4.0 mL, 21.9 mmol, E. Merck) in CH_2Cl_2 under nitrogen.[20] The solution was refluxed at 50 °C with stirring for 7 h. After evaporation followed by neutralization with Et_3N, the product was chromatographed on silica gel to examine the progress of the reaction. The reaction mixture was mixed with 1-dodecanol (3.6 mL, 15.5 mmol, Wako Pure Chemicals), $BF_3{\cdot}OEt_2$ (21 mL, 7.9 mmol, Wako Pure Chemicals) in the presence of 4 Å molecular sieves (2.5 g), and stirred at room temperature for 22 h.[21] $BF_3{\cdot}OEt$ (20.1 mL, 0.79 mmol) was added at 18 h to complete the reaction. The mixture was neutralized with Et_3N. After evaporation, the product was purified by column chromatography (Silica Gel 60, E. Merck, 7 × 30 cm, 1:1 *n*-hexane–EtOAc). Yield: 63.8% (2.53 g). ^{1}H NMR($CDCl_3$): δ 5.51 (d, 1H, $J_{2,NH}$ 8.8 Hz, NH), 5.31 (dd, 1H, $J_{2,3}$ 10.1 Hz, $J_{3,4}$ 9.5 Hz, H-3), 5.06 (dd, 1H, $J_{3,4}$ 9.5 Hz, $J_{4,5}$ 9.9 Hz, H-4), 4.65 (d, 1H, $J_{1,2}$ 8.4 Hz, H-1), 4.26 (dd, 1H, $J_{5,6b}$ 4.7 Hz, $J_{6,gem}$ 12.3 Hz, H-6a), 4.12 (dd, 1H, $J_{5,6a}$ 2.4 Hz, $J_{6,gem}$ 12.3 Hz, H-6b), 3.89–3.75 (m, 2H, $J_{2,NH}$ 8.8 Hz, $J_{1,2}$ 8.4 Hz, H-2, $OCH_2CH_2(CH_2)_9CH_3$), 3.69 (ddd, $J_{4,5}$ 9.9 Hz, $J_{5,6a}$ 2,4 Hz, $J_{5,6b}$ 4.7 Hz, H-5), 3.50–3.42 (m, 1H, $OCH_2CH_2(CH_2)_9CH_3$), 1.94, 2.02, 2.02, and 2.08 (s, each 3H, Ac), 1.60–1.50 (m, 2H, OCH_2CH_2-$(CH_2)_9CH_3$), 1.35–1.14 (m, 18H, $OCH_2CH_2(CH_2)_9CH_3$), 0.87 (t, 3H,$OCH_2CH_2(CH_2)_9CH_3$).

Dodecyl 2-acetamido-3,4,6-tri-*O*-acetyl-2-deoxy-β-D-glucopyranoside (2.5 g, 4.85 mol) in 100 mL of MeOH was deacetylated in the presence of NaOMe (270 mg, 5.0 mmol, Wako Pure Chemicals). Deprotection was carried out with stirring for 40 min. After decolorization on charcoal in EtOH, the product GlcNAc-C12 was obtained by recrystallization in ethanol. Yield: 1.70 g (88.1%). Mp 160–162 °C, lit.[22] mp 161 °C, $[\alpha]_D$ −18.8 (*c* 0.12, CH_3OH). ^{1}H NMR (CD_3OD): δ 4.38 (d, 1H, $J_{1,2}$ 6.1 Hz, H-1), 3.91–3.83 (m, 2H, H-6a, NH), 3.70–3.58 (m, 2H, H-2, H-5), 3.48–3.40 (m, 2H, H-3, H-6b), 3.34–3.27 (m, 3H, H-4, OCH_2), 1.97 (s, 3H, Ac), 1.53–1.51 (m, 2H, $OCH_2CH_2(CH_2)_9CH_3$), 1.34–1.22 (m, 18H, $OCH_2CH_2(CH_2)_9CH_3$), 0.89 (t, 3H, OCH_2CH_2-$(CH_2)_9CH_3$). MALDI-TOFMS: calcd for $C_{20}H_{39}NO_6$: $(M+Na)^+$, 412.3, Found: $(M+Na)^+$, 412.3. Anal. Calcd for $C_{20}H_{39}NO_6{\cdot}0.3H_2O$ (398.68): C, 60.82; H, 10.11; N, 3.55. Found: C, 60.81; H, 10.04; N, 3.54.

4.2. Synthesis of dodecyl β-D-galactopyranosyl-(1→4)-2-acetamido-2-deoxy-β-D-glucopyranoside (LacNAc-C12)

2,3,4,6-Tetra-*O*-acetyl-β-D-galactopyranosyl-(1→4)-2-acetamido-1,3,6-tri-*O*-acetyl-2-deoxy-β-D-glucopyranoside (Ac-LacNAc) was prepared by mixing *N*-acetyllactosamine (982 mg, 2.56 nmol, LacNAc, Yaizu Suisankagaku Industry Co. Ltd, Japan) with Ac_2O (5 mL, 52.9 mmol) in 10 mL of pyridine. Ac-LacNAc (0.799 g, 1.88 mmol) was mixed with TMS-OTf (0.24 mL, 1.33 mmol) in CH_2Cl_2 under nitrogen. The solution was refluxed at 50 °C with stirring for 12 h. After evaporation, followed by neutralization with Et_3N, the product was chromatographed on silica gel to examine the progress of reaction. After evaporation, the product was collected by column chromatography (Silica Gel 60, 2 × 23 cm, 1:2:0.01 toluene–EtOAc–Et_3N). The collected products were mixed with 1-dodecanol (1.3 mL, 5.89 mmol), (*R*,*S*)-camphor sulfonate (27 mg, 0.12 mmol, Wako Pure Chemicals) in the presence of 4 Å molecular sieves (350 mg), and refluxed for 6 h. The mixture was neutralized with Et_3N. After evaporation of the solvent, the product was purified by column chromatography (Silica Gel 60, 2 × 35 cm, 2:3 *n*-hexane–EtOAc). Yield: 50% (478 mg). ^{1}H NMR ($CDCl_3$): δ: 5.63 (d, 1H, $J_{NH,2}$ 9.3 Hz, NH), 5.35 (d, 1H, $J_{3',4'}$ 2.9 Hz, H-4′), 5.11 (dd, 1H, H-2′), 5.06 (dd, 1H, $J_{3,4}$ 8.1 Hz, H-3), 4.97 (dd, 1H, $J_{2',3'}$ 10.3 Hz, H-3′), 4.51–4.46 (m, 2H, H-1′, H-6a), 4.43 (d, 1H, $J_{1,2}$ 7.3, H-1), 4.15–4.09 (m, 3H, H-6b, H-6b′, H-6a′), 4.03 (dd, 1H, $J_{2,3}$ 9.3 Hz, H-2), 3.87 (ddd, 1H, H-5′), 3.78 (dd, 1H, H-4), 3.62 (ddd, 1H, $J_{4,5}$ 5.6 Hz, H-5), 3.41 (dd, 2H, $OCH_2CH_2(CH_2)_9CH_3$), 2.15–1.96 (m, 21H, Ac), 1.60–1.46 (m, 2H, $OCH_2CH_2(CH_2)_9CH_3$), 1.30–1.18 (m, 18H, $OCH_2CH_2(CH_2)_9CH_3$), 0.87 (t, 3H, $OCH_2(CH_2)_{10}CH_3$).

Dodecyl 2,3,4,6-tetra-*O*-acetyl-β-D-galactopyranosyl-(1→4)-2-acetamido-3,6-di-*O*-acetyl-2-deoxy-β-D-glucopyranoside (478 g, 0.56 mmol) in 25 mL of MeOH was deacetylated by the addition of NaOMe (160 mg, 2.97 mmol) with stirring for 3 h. The reactant was concentrated after treating with Amberlite IR-120B (Organo Co., Japan). LacNAc-C12 was purified by distilling with EtOH, toluene, and $CHCl_3$. Yield: 326 mg

(99%). mp 246 °C, $[\alpha]_D$ −7.6 (*c* 0.2, DMSO). ^{1}H NMR(DMSO-d_6): δ 7.74 (d, 1H, NH), 4.28 (d, 1H, $J_{1,2}$ 7.8 Hz, H-1′), 4.19 (d, 1H, $J_{1,2}$ 8.1 Hz, H-1), 1.7 (s, 3H, Ac), 1.42–1.41 (m, 2H, $OCH_2CH_2(CH_2)_9CH_3$), 1.17–1.29 (m, 18H, $OCH_2CH_2(CH_2)_9CH_3$), 0.85 (t, 3H, $OCH_2CH_2(CH_2)_9CH_3$). MALDI-TOFMS: calcd for $C_{26}H_{49}NO_{11}$: $(M+Na)^+$, 574.3, found: $(M+Na)^+$, 574.6. Anal. Calcd for $C_{26}H_{49}NO_{11}\cdot 1.5H_2O$ (578.35): C, 53.96; H, 9.06; N, 2.42. Found: C, 54.24; H, 8.77; N, 2.30.

4.3. Cell culture

HL-60 cells (Riken Cell Bank) were grown in RPMI 1640 medium (Nissui Pharm. Co., Ltd) supplemented with 10% heat-inactivated fetal bovine serum (JRH Biosciences Inc.) at 37 °C in humidified 5% CO_2. B16 cells (Riken Cell Bank) were grown in DMEM (Gibco BRL) supplemented with streptomycin 0.1 g/L, penicillin G potassium 50,000 unit/L, and 10% heat-inactivated fetal bovine serum (JRH Biosciences Inc.) at 37 °C in humidified 5% CO_2.

4.4. Glycosylation of saccharide primers in cells

Stock solutions of 20 mM saccharide primers in DMSO were diluted to 50 μM with serum-free and phenol red-free culture medium consisting of RPMI 1640 medium (Gibco BRL) containing 5 mg/L of transferrin, 5 mg/L of insulin, and 30 nM selenium dioxide.

Glycosylation by cells was carried out as follows: HL60 cells (2×10^6) were incubated with RPMI 1640 medium containing 50 μM saccharide primer for 48 h. The glycosylated products secreted in the culture medium were collected with a Sep-Pak C_{18} column (Waters Co.). The water-soluble compounds were removed with water and 3:7 MeOH–H_2O. The glycosylated products were eluted with MeOH. The eluate containing the glycosylated products was evaporated under reduced pressure. The obtained products were dissolved in 100 μL of 2:1 $CHCl_3$–MeOH, and an aliquot was separated on an HPTLC plate (Silica Gel 60, E. Merck) using $CHCl_3$–MeOH–0.2% $CaCl_2$. Acidic and neutral products on the HPTLC plate were stained with resorcinol–HCl reagent and orcinol–H_2SO_4 reagent, respectively. B16 cells (2×10^6) were similarly incubated with saccharide primers in serum-free DMEM/F-12 medium (Gibco BRL) containing 5 mg/L of transferrin, 5 mg/L of insulin, and 30 nM selenium dioxide.

4.5. TLC blotting

TLC blotting was carried out as follows: Glycosylated products separated on an HPTLC plate were sprayed with primuline reagent, and the spots were marked with a red pencil under UV light. Then, the HPTLC plate was dipped in a blotting solvent of 40:7:20 2-PrOH–MeOH–0.2% $CaCl_2$ for 20 s and placed on a glass fiber filter (ATTO Co.). The plate was covered with a PVDF membrane (ATTO Co.), a PTFE membrane (ATTO Co.), and another glass fiber filter. These layers were subjected to pressure at 180 °C for 30 s using a TLC thermal blotter (ATTO Co.). The PVDF membrane was washed with pure water, and glycolipid fractions were extracted with MeOH and 2:1 $CHCl_3$–MeOH.

4.6. High-performance liquid chromatography (HPLC)

Neutral products and acidic products separated using a Sep-Pak C_{18} column were purified by HPLC. The crude products dissolved in 70:28:2 $CHCl_3$–MeOH–H_2O were injected into an HPLC system equipped with an Iatrobead column (6RSP-8005, 4.6 × 250 mm, Iatron Laboratories Inc.) and a light scattering detector (SEDEX75, Sedere). Neutral products were separated with 70:28:2 $CHCl_3$–MeOH–H_2O. Acidic products were separated with 70:28:2 $CHCl_3$–MeOH–H_2O and 60:35:5 $CHCl_3$–MeOH–H_2O. The flow rate was 2 mL/min. The fractions were collected at 30-s intervals for 40 min.

4.7. Mass spectrometry

The structural analyses of glycosylated products were carried out by a MALDI-TOF mass spectrometer (Autoflex, Bruker Daltonics) and an ESI mass spectrometer (Esquire 3000, Bruker Daltonics). 2,5-Dihydroxybenzoic acid (DHB, Aldrich) was employed as a matrix.

4.8. Digestion of glycosylated products by enzymes

Enzymatic digestion of glycosylated products was carried out in 50 mM NaOAc buffer (pH 4.8) containing 50 mU of neuraminidase from *A. ureafaciens* (EC.3.2.1.18, Sigma), or in 50 mM sodium acetate butter (pH 5.5) containing 10 mU of neuraminidase from *M. decora* (EC. 3.2.1.18, Calbiochem). The reactions were carried out in the presence of 0.6 mg/mL sodium taurodeoxycholic acid. The products were collected using a Sep-Pak C_{18} column, separated on an HPTLC plate with 60:35:8 $CHCl_3$–MeOH–0.2% $CaCl_2$, and were stained with orcinol–H_2SO_4.

4.9. MTT assay

Cells (2×10^4) in a 96-well microplate were incubated with 50 μM GlcNAc-C12 or LacNAc-C12 for 48 h. Ten μL of WST-1 dye solution (10 mM WST-1 and 0.2 mM 1-methoxy PMS, Dojindo Laboratories) per well was added to each well. After 2 h, absorbance at 450 nm with a reference wavelength of 690 nm was measured using a microplate reader (Multiskan, Labsystem).

Acknowledgments

This work was partly supported by funds from the Program for Promotion of Basic Research Activities for Innovative Biosciences, and the Special Coordination of Funds for Promoting Science and Technology from the Ministry of Education, Culture, Sports, Science and Technology, the Japanese Government (T.S.).

Supplementary data

Supplementary data associated with this article can be found, in the online version, at doi:10.1016/j.carres.2008.01.022.

References

1. Miura, Y.; Yamagata, T. *Biochem. Biophys. Res. Commun.* **1997**, *241*, 698–703.
2. Nakajima, H.; Miura, Y.; Yamagata, T. *J. Biochem.* **1998**, *124*, 148–156.
3. Okayama, M.; Kimata, K.; Suzuki, S. *J. Biochem.* **1973**, *74*, 1069–1073.
4. Schwartz, N. B. L.; Galligani, P.-L. Ho.; Dorfman, A. *Proc. Natl. Acad. Sci. U.S.A.* **1974**, *71*, 4047–4051.
5. Sarkar, A. K.; Fritz, T. A.; Taylor, W. H.; Esko, J. D. *Proc. Natl. Acad. Sci. U.S.A.* **1995**, *92*, 3323–3327.
6. Sarkar, A. K.; Rostand, K. S.; Jain, R. K.; Matta, K. L.; Esko, J. D. *J. Biol. Chem.* **1997**, *272*, 25608–25616.
7. Yamagaki, T.; Nakanishi, H. *J. Mass Spectrom.* **2000**, *35*, 1300–1307.
8. Handa, K.; Withers, D.-A.; Hakomori, S. *Biochem. Biophys. Res. Commun.* **1998**, *243*, 199–204.
9. Nishihara, S.; Iwasaki, H.; Kaneko, M.; Tawada, A.; Ito, M.; Narimatsu, H. *FEBS Lett.* **1999**, *462*, 289–294.
10. Saito, M.; Sugano, K.; Nagai, Y. *J. Biol. Chem.* **1979**, *254*, 7845–7854.
11. Chou, M.-Y.; Li, S.-C.; Kiso, M.; Hasegawa, A.; Li, Y.-T. *J. Biol. Chem.* **1994**, *269*, 18821–18826.
12. Pan, G. G.; Melton, L. D. *J. Chromatogr.* **2005**, *1077*, 136–142.
13. Stroud, M.-R.; Holmes, E.-H. *Biochem. Biophys. Res. Commun.* **1997**, *238*, 165–168.
14. Stroud, M.-R.; Handa, K.; Salyan, M.-E.-K.; Ito, K.; Levery, S.-B.; Hakomori, S. *Biochemistry* **1996**, *35*, 758–769.
15. Kasuya, M. C. Z.; Wang, L. X.; Lee, Y. C.; Mitsuki, M.; Nakajima, H.; Miura, Y.; Sato, T.; Hatanaka, K.; Yamagata, S.; Yamagata, T. *Carbohydr. Res.* **2000**, *329*, 755–763.
16. Sato, T.; Fujita, S.; Kasuya, M. C. Z.; Hatanaka, K.; Yamagata, T. *Chem. Lett.* **2004**, *33*, 580–581.
17. Nojiri, H.; Takaku, F.; Tetsuka, T.; Motoyoshi, K.; Miura, Y.; Saito, M. *Blood* **1984**, *64*, 534–541.
18. Sato, T.; Hatanaka, K.; Hashimoto, H.; Yamagata, T. *Trends Glycosci. Glycotechnol.* **2007**, *19*, 1–17.
19. Horton, D. *J. Org. Chem.* **1964**, *29*, 1776–1782.
20. Nakabatashi, S.; Warren, C. D.; Jeanlozs, R. W. *Carbohydr. Res.* **1986**, *150*, C7–C10.
21. Xia, J.; Piskorz, C. F.; Locke, R. D.; Chandrasekaran, E. V.; Alderfer, J. L.; Matta, K. L. *Bioorg. Med. Chem. Lett.* **1999**, *9*, 2941–294622.
22. Boullanger, P.; Chevalier, Y.; Croizier, M.-C.; Lafont, D.; Sancho, M.-R. *Carbohydr. Res.* **1995**, *278*, 91–101.

Selection of a Carbohydrate-Binding Domain with a Helix−Loop−Helix Structure[†]

Teruhiko Matsubara,[‡] Mie Iida,[‡] Takeshi Tsumuraya,[§] Ikuo Fujii,[§] and Toshinori Sato*[,‡]

Department of Biosciences and Informatics, Faculty of Science and Technology, Keio University, 3-14-1 Hiyoshi, Kouhoku-ku, Yokohama 223-8522, Japan, and Department of Biological Science, Graduate School of Science, Osaka Prefecture University, 1-2 Gakuen-cho, Sakai, Osaka 599-8570, Japan

Received January 16, 2008; Revised Manuscript Received March 19, 2008

ABSTRACT: We obtained a novel carbohydrate-binding peptide having a helix−loop−helix scaffold from a random peptide library. The helix−loop−helix peptide library randomized at five amino acid residues was displayed on the major coat protein of a filamentous phage. Affinity selection with a ganglioside, Galβ1−3GalNAcβ1−4(Neu5Acα2−3)Galβ1−4Glcβ1−1′Cer (GM1), gave positive phage clones. Surface plasmon resonance spectroscopy showed that a corresponding 35-mer synthetic peptide had high affinity for GM1 with a dissociation constant of 0.24 μM. This peptide preferentially binds to GM1 rather than asialo GM1 and GM2, suggesting that a terminal galactose and sialic acid are required for the binding as for cholera toxin. Circular dichroism spectroscopic studies indicated that a helical structure is important for the affinity and specificity. Furthermore, alanine scanning at randomized positions showed that arginine and phenylalanine play an especially important role in the recognition of carbohydrates. Such a de novo helix−loop−helix peptide would be available for the design of carbohydrate-binding proteins.

Lectins, antibodies, and proteins which are specific to carbohydrates serve as powerful tools in the identification of the physiological roles of glycoconjugates (*1*). Despite this, because glycotopes are poor immunogens, it is difficult to obtain antiglycan and antiglycolipid antibodies (*2*, *3*). Approximately two-thirds of carbohydrate-binding antibodies are IgM (*2*), their affinity and specificity not always being sufficient in clinical use as a glycan probe. To overcome this, the affinity of antibodies has been improved through selection from phage-display libraries over the past decade (*4*). The affinity of monoclonal antibodies against oligosaccharides of Lewis^X (*5*), sialyl Lewis^X (*6*), α-galactosyl epitope (*7*), Thomsen-Friedenreich antigen (*8*), Galβ1−3GalNAcβ1−4Galβ1−4Glcβ1−1′Cer (asialo GM1)[1] (*3*), and Neu5Gcα2−3Galβ1−4Glcβ1−1′Cer (*N*-glycoyl GM3) (*9*) has improved. When it comes to lectin (*10*, *11*) and hemagglutinin (*12*, *13*), attempts to change binding specificity through mutation have been reported.

An alternative strategy might have great potential in the engineering of tailor-made artificial carbohydrate-binding proteins. Research groups have adopted various structural motifs for the de novo design of polypeptides such as metalloproteins (*14*), catalysts (*15*, *16*), and bacteriorhodopsin (*17*). Random library-based selection and evolution with structural scaffolds using display technologies have provided proteins that target specific molecules (*18*, *19*). In this study, a stable helix−loop−helix structure was chosen to construct an artificial carbohydrate-binding domain. Helix-based motifs are frequently conserved in proteins during molecular evolution (*20*). Selection from a randomized peptide library with the helix-type scaffold would give peptides that play a role as a carbohydrate-binding domain.

The ganglioside GM1 is well-known as a receptor of cholera toxin B subunit (CTB) (*21*, *22*) and is often used as a marker of lipid rafts (*23*). Yanagisawa noted that GM1 is correlated with the accumulation of β-amyloid in cases of Alzheimer's disease (*24*). The development of GM1-binding molecules is required for investigation of the localization and roles of GM1 on the cell surface. Our previous selection from a random library showed a pentadecapeptide, p3, with affinity for a GM1 pentasaccharide with a dissociation constant (K_d) of 1.2 μM (*25*, *26*). This peptide was specific to GM1 as well as CTB, but the binding affinity of the peptide was lower than that of CTB ($K_d = 10^{-8}$–10^{-12} M) (*22*). Two-dimensional nuclear magnetic resonance (NMR) experiments showed that a conformational change of this peptide occurred during the binding to GM1 (*27*). To decrease the entropic loss caused by the conformational change, a helix-type scaffold was adopted for the selection. Five amino acids at the C-terminal helix of the helix−loop−helix scaffold were randomized to identify the GM1-specific peptide sequences. Phage display selection, alanine scanning, and circular dichroism experiments indicated the peptide to be specific

[†] This work was supported by a Grant-in-aid for the Encouragement of Young Scientists (17750166, T.M.) from the Ministry of Education, Culture, Sports, Science and Technology of the Japanese Government.

* To whom correspondence should be addressed: Department of Biosciences and Informatics, Faculty of Science and Technology, Keio University, 3-14-1 Hiyoshi, Kouhoku-ku, Yokohama 223-8522, Japan. Phone: +81-45-566-1771. Fax: +81-45-566-1447. E-mail: sato@bio.keio.ac.jp.

[‡] Keio University.

[§] Osaka Prefecture University.

[1] Abbreviations: GSL, glycosphingolipid; GM1, Galβ1−3GalNAcβ1−4(Neu5Acα2−3)Galβ1−4Glcβ1−1′Cer; GM2, GalNAcβ1−4(Neu5Acα2−3)Galβ1−4Glcβ1−1′Cer; asialo GM1, Galβ1−3GalNAcβ1−4Galβ1−4Glcβ1−1′Cer; GlcCer, Glcβ1−1′Cer; CTB, cholera toxin B subunit; K_d, dissociation constant; NMR, nuclear magnetic resonance; CFU, colony-forming units; PBS, phosphate-buffered saline; TBS, Tris-buffered saline; BSA, bovine serum albumin; ELISA, enzyme-linked immunosorbent assay; CD, circular dichroism; SPR, surface plasmon resonance; RU, resonance units; R_{max}, maximum resonance; R_{eq}, equilibrium resonance units; Δ*G*, Gibbs free energy change.

10.1021/bi8000837 CCC: $40.75
Published on Web 06/10/2008

to GM1 and the helical conformation to be necessary for the specific binding.

EXPERIMENTAL PROCEDURES

Materials. Gangliosides and glycosphingolipids (GSLs), Galβ1−3GalNAcβ1−4(Neu5Acα2−3)Galβ1−4Glcβ1−1′Cer (GM1), GalNAcβ1−4(Neu5Acα2−3)Galβ1−4Glcβ1−1′Cer (GM2), Galβ1−3GalNAcβ1−4Galβ1−4Glcβ1−1′Cer (asialo GM1), and Glcβ1−1′Cer (GlcCer) were obtained from Sigma-Aldrich Co. (St. Louis, MO). Anti-fd bacteriophage antibody, peroxidase-conjugated anti-rabbit IgG antibody, and peroxidase-conjugated cholera toxin B subunit (CTB) were obtained from Sigma-Aldrich. XL1-blue cell and helper phage (VCSM13) were obtained from Stratagene Co. (La Jolla, CA).

Phage Display Library. A random library of a helix−loop−helix peptide, AELAALEAELAALE-G_7-KLXXLKXKLXX-LKA, was constructed using a pComb8 system (*28*). This library was displayed on major coat protein VIII of a filamentous phage with a GGSSA spacer and GAPVPYP-DPLEPR (E-tag). We estimated the library has 3.2×10^7 recombinants, which is enough diversity to cover five randomized amino acids ($20^5 = 3.2 \times 10^6$).

Affinity Selection with GM1. For affinity selection, a ganglioside GM1 monolayer was prepared at the air−water interface in a Langmuir trough and immobilized onto a plastic plate (code 174950, Nunc) as reported previously with a minor modification (*25, 26*). The phage library (5×10^9 CFU) was incubated with GM1 in 200 μL of phosphate-buffered saline (PBS) at pH 6.0 ([phage] = 0.041 nM). After 30 min, the GM1 plate was washed three times to remove unbound phages. Bound phages were eluted for 15 min with glycine-HCl buffer (pH 2), and the eluate was neutralized with Tris-HCl buffer at pH 9.1. To estimate the phage number collected, a small portion of the eluate was saved and used for titering. *Escherichia coli* XL1-blue cells were infected with the phages in SB medium incubated for 30 min at 37 °C. After the addition of ampicillin, the transformed cells were grown for 1 h at 37 °C. The phages were rescued by adding a VCSM13 helper phage and further amplified overnight. The phages amplified were collected and purified with polyethylene glycol and NaCl for the next round. This process was repeated seven or nine times. After the last round of affinity selection, the titering plate was used to isolate individual phage clones. Each phagemid cloned was purified with a QIAprep Spin Miniprep Kit (QIAGEN Inc.) and used as a template for sequencing to deduce the amino acid sequence.

Peptide Synthesis and Purification. Peptides (peptide amides) were synthesized with a solid-phase peptide synthesizer (model 433A, Applied Biosystems) using 9-fluorenylmethoxycarbonyl (Fmoc) chemistry. The peptides were purified by reversed-phase high-performance liquid chromatography (C_{18} column, 250 mm × 20 mm inside diameter) with a linear gradient of water containing 0.1% trifluoroacetic acid (TFA) and acetonitrile containing 0.1% TFA at a flow rate of 10 mL/min. The major fractions were lyophilized, and the peptides were characterized by matrix-assisted laser desorption ionization time-of-flight mass spectrometry (autoflex, Bruker Daltonics, Inc.) using a matrix of α-cyano-4-hydroxycinnamic acid.

Circular Dichroism (CD) Spectroscopy. CD spectroscopy was performed on a Jasco J-820 spectropolarimeter using a 1 mm cuvette. Spectra were collected from 260 to 190 nm every 0.2 nm. The peptide concentrations were determined by measuring tyrosine absorbance (the molar absorbance coefficient at 257 nm equals 1450 M^{-1} cm^{-1}). A peptide solution (100 μM) was prepared with Tris-buffered saline (TBS) (50 mM Tris-HCl and 150 mM NaCl) at pH 7.5. The CD spectra are reported as mean residue ellipticity ([θ]) in degrees per square centimeter per decimole. The α-helical content was calculated from the following equation (*29*).

$$\alpha\text{-helical content} = (-[\theta]_{222} + 2340)/30300$$

Surface Plasmon Resonance (SPR) Analysis. The affinity of peptides for glycolipids was determined by SPR using a Biacore X biosensor system (Biacore International). The glycolipid monolayer was immobilized on a bare gold sensor chip (code BR-1004-05, Biacore International), and this chip was docked into the instrument. All measurements were carried out in TBS (pH 7.5) which was filtered (0.22 μm) and degassed prior to use. After the docking, TBS was injected over the chip at a flow rate of 10 μL/min for 30−40 min. Analyses were performed at 25 °C and with a flow rate of 5 μL/min for the determination of equilibrium binding. The sensor chip surfaces were regenerated with 4 M $MgCl_2$ for 8 min.

Binding affinity was calculated from a Scatchard analysis of equilibrium binding using the equation

$$R_{eq}/[\text{peptide}] = R_{max}/K_d - R_{eq}/K_d$$

where [peptide], R_{max}, and K_d are the concentration of peptide, the maximum resonance, and the dissociation constant, respectively. The resonances in the association phase at 500−600 s were used as the equilibrium resonance units (R_{eq}). The average R_{eq} values were plotted in the form R_{eq}/[peptide] versus R_{eq}, and K_d and R_{max} were calculated from the slope and intercept of the linear relationship, respectively. The peptide concentration range (1−20 μM) in which the peptide amounts were analyzed as a single interaction by a Scatchard plot was used to determine K_d values. In the case of B72, the concentrations of 1−10 μM were used for the analysis, since the multilayer adsorption was observed at 20 μM and reliable signals were not detected below 1 μM.

Molecular Modeling. Molecular modeling was performed using the InsightII/Discover3 system (Accelrys, Inc.). The peptide amide Ct5 was built using the Biopolymer module in InsightII, where the main chains of 1−14 and 22−36 residues are taken as the helical structure and the chain of 15−21 residues is extended. Simple minimization was performed using Discover3. To obtain peptide B72, substitutions of four alanines with Lys24, Arg28, Arg31, and Phe32 were made in Ct5 using the Biopolymer module. After the minimization, the final structure was used for the drawing shown in Figure 8. Crystallographic coordinates of the X-ray structure of pentasaccharide GM1 were obtained from the Protein Data Bank (entry 3CHB). The B72 peptide and GM1 pentasaccharide were superimposed.

RESULTS

Helix−Loop−Helix Design. The helix−loop−helix scaffold is composed of two helical sequences with seven

FIGURE 1: Structure of the helix−loop−helix library. An illustration of the helix−loop−helix library is shown at the left. Five randomized positions are arranged in the C-terminal helix, where X is a randomized position. The amino acid sequence of the helix−loop−helix peptide library is shown at the right.

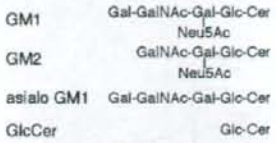

FIGURE 2: Schematic representation of gangliosides and GSLs employed in this study. Glc, glucose; Gal, galactose; GalNAc, *N*-acetylgalactosamine; Neu5Ac, *N*-acetylneuraminic acid; Cer, ceramide.

glycines as a spacer (Figure 1) (*30*). Leucines, glutamic acids, and lysines were positioned to stabilize the helical structure through hydrophobic interaction and the formation of salt bridges. We prepared a helix−loop−helix library for phage display selection with random substitutions at positions 24, 25, 28, 31, and 32 (*31*). The substituted residues were positioned outside of the C-terminal helix.

Phage Display Selection against GM1. The selection of peptides with affinity for ganglioside GM1 (Figure 2) was carried out as reported with minor revisions (*25*). Briefly, a GM1 monolayer was prepared at the air−water interface with a Langmuir trough and transferred to a plastic plate. The phage library was incubated with GM1 on the plate, and the bound phages were eluted under acid conditions. The phages obtained were amplified, purified, and subjected to another round. After seven and nine rounds of selection, 16 and 20 clones were isolated, respectively. The phage ELISA was used to identify the clones that have affinity for GM1 (Supporting Information, Figure S1). The first screening of 36 phage clones was performed via an ELISA, and then 13 clones were chosen for further investigation. To know the binding selectivity of 13 clones, K_d values for GM3 and GalCer were also investigated (data not shown). A914 and B72 were found to have high affinity for GM1 with K_d values of 0.075 and 0.13 nM, respectively, and exhibited a higher affinity than for GM3 and GalCer (Supporting Information, Table S1).

Binding Affinity and Helical Structure of Peptides. To analyze their affinity, these peptides were chemically synthesized (C-terminus amidated). To estimate the peptide concentration in buffer, tyrosine was added at the C-terminus of the peptide (Table 1). The binding of these peptides was characterized by the surface plasmon resonance method. Figure 3A shows typical sensorgrams of peptides A914, B72, and Ct5 at 10 μM in TBS (pH 7.5). Ct5 is a control peptide in which all sites randomized in the library are changed to alanines. The amount of B72 bound to GM1 was greater than that of other peptides and increased as the peptide concentration increased (Figure 3B). However, the kinetics of binding was not analyzed due to the rapid association and dissociation phases observed. Then, equilibrium binding experiments were performed to calculate K_d values using Scatchard plots; the K_d was 2.9 μM for A914, 0.24 μM for B72, and 11 μM for Ct5 (Table 1 and Figure 4). The binding affinity of B72 was 25-fold higher than that of the control Ct5. The R_{max} values for B72, Ct5, and B72-h, which is the C-terminal half of B72 containing five residues identified, were 280, 268, and 145 RU, respectively. These amounts bound to GM1 approximately corresponded to their molecular weights. However, A914 showed low affinity (2.9 μM) and small amounts (151 RU) against GM1, though the A914 phage clone had the same affinity for GM1 as the B72 clone (Table S1). Such a discrepancy between synthetic peptides and phage clones is often observed (*25*, *32*). The binding preference of the selected peptides depends on the method of measurement. Then, on the basis of the results in Table 1, we chose B72 for further characterization. The K_d value of a 15-mer peptide, p3, selected previously was 1.2 μM (*26*). B72 exhibited greater (5-fold) affinity for GM1 than the nonhelical peptide p3. Lectins, toxins, and antibodies have several carbohydrate-binding domains (*33*). A multivalent B72 as tandem repeats or tentacle-type multimers would enhance the binding affinity (*34*).

To clarify how the helix of B72 is affected upon carbohydrate recognition, the secondary structure of B72 was investigated by CD spectroscopy. The CD spectra of B72 and Ct5 exhibited two minima at 208 and 222 nm, indicating a typical α-helical structure (Figure 5) (*35*). The mean residue ellipticity at 222 nm was −10471 deg cm^2 dmol^{-1} for B72 and −16040 deg cm^2 dmol^{-1} for Ct5. The helical content was estimated to be 42% for B72 and 61% for Ct5 (*29*). B72-h took no helical structure and had a lower affinity (K_d = 5.0 μM) than full-length B72 (K_d = 0.24 μM) (Table 1). These results suggest that the binding of B72 to GM1 was influenced by its secondary structure.

Binding Specificity of Peptides. The specificity with which B72, Ct5, and B72-h bind various glycolipids is shown in Figure 6 and summarized in Table 2. The affinity of B72 was 0.016- and 0.073-fold lower for GM2 and asialo GM1 than for GM1, respectively (15 μM for GM2 and 3.3 μM for asialo GM1). The binding preference (GM1 ≫ asialo GM1 > GM2) of B72 was in good agreement with that of p3 (*26*). The profile of the binding of Ct5 to GM1 was no different from that of the binding to other glycolipids, and the amount of B72-h bound to GM1 declined to the same level as that bound to GlcCer (as nonspecific binding) (Figure 6). These results suggested that the helical conformation and the five residues in B72 were crucial for the specificity for GM1.

Alanine Scanning. To determine the contribution of the five residues in B72, four alanine-substituted mutants of B72 were synthesized (B72-1, B72-2, B72-3, and B72-4) (Table 3). Single-alanine substitutions at positions 24, 28, 31, and 32 are predicted to alter the GM1 binding profile and helical conformation. The amount of peptide bound to GM1 was affected by all alanine substitutions (Table 3, Figure 7A, and Figure S2). Notably, the replacement of Arg31 (B72-3) and Phe32 (B72-4) with Ala markedly decreases the affinity for GM1; the amounts of B72-3 (67 RU at 5 μM) and B72-4 (54 RU) were 4−5-fold smaller than the amount of B72 (261 RU). The amounts of these mutants decreased to the same level as the control peptide, Ct5 (80 ± 23 RU at 5 μM) (Figure 6). It was suggested that Arg31 and Phe32 among

Table 1: Affinity of Synthetic Peptides for GM1

code	peptide structure [a]	molecular weight	R_{max} (RU)	K_d (μM)	relative affinity [b]
A914	AELAALEAELAALEGGGGGGGKLQELKTKLAALKAY-NH_2	3512.02	151	2.9	0.083
B72	AELAALEAELAALEGGGGGGGKLKALKRKLRFLKAY-NH_2	3670.31	280	0.24	1.0
B72-h	GGGKLKALKRKLRFLKAY-NH_2	1743.14	145	5.0	0.048
Ct5	AELAALEAELAALEGGGGGGGKLAALKAKLAALKAY-NH_2	3366.90	268	11	0.022

[a] Random positions are underlined. [b] Ratio to B72 peptide.

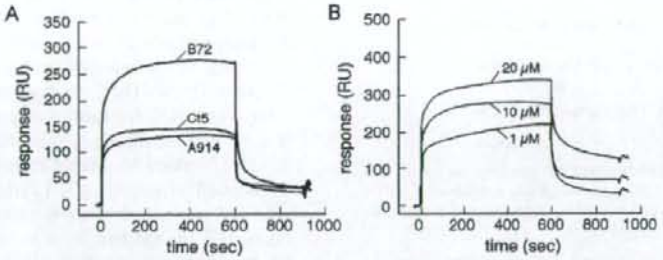

FIGURE 3: SPR sensorgrams for the interaction of peptides with GM1. (A) Overlay plot of the binding of A914, B72, and Ct5 at 10 μM. (B) Overlay plot of the binding of B72 at 1, 10, and 20 μM. Responses in RU are plotted vs time in seconds. Association (0−600 s) and dissociation (600−900 s) phases are shown.

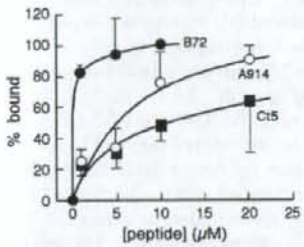

FIGURE 4: Amounts of A914, B72, and Ct5 bound to GM1 at various peptide concentrations observed by SPR spectroscopy. % bound, $(R_{eq}/R_{max}) \times 100$; R_{eq}, equilibrium response units at 500−600 s in the association phase; R_{max}, maximum response calculated from Scatchard plots (data not shown). The data are average values ± the standard deviation ($n = 2-4$).

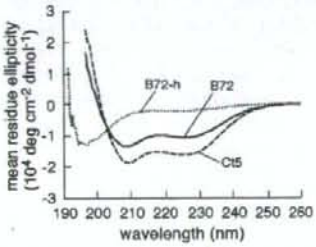

FIGURE 5: CD spectra of B72 (—), B72-h (•••), and Ct5 (---) in TBS at pH 7.5. The peptide concentration was 100 μM.

the four amino acid residues strongly contributed to the binding. In our previous studies, arginines and hydrophobic amino acids had been found in the motif shared among GM1-binding peptides (*25*, *26*). These results were consistent with our previous papers.

To determine the influence of alanine substitutions on the helical conformation, CD spectra of these mutants were measured (Figure 7B). The two maxima at 208 and 222 nm were found in all the mutants, which indicates that the helical structure was maintained. The mean residue ellipticity at 222 nm of B72 mutants decreased except for that of B72-2; indeed, the α-helical content increased (65, 34, 59, and 48% for B72-1, B72-2, B72-3, and B72-4, respectively). Alanine is a stabilizer of helices, so an enhancement of helicity with alanine substitutions is reasonable (*36*). The CD spectra indicated that the decreases in affinity for GM1 are due to the loss of side chains of residues identified, and not due to disruption of the helical conformation.

DISCUSSION

The development of carbohydrate-binding molecules like lectins, toxins, and antibodies would greatly contribute to the evolution of glycoscience and glycotechnology. Especially for functional analyses of glycoconjugates, the need for carbohydrate-binding molecules will increase with progress in glycobiology (*37*−*41*). Recently developed selection technology, including the use of genomic and random libraries, has provided various repertories of carbohydrate-binding molecules (*42*). Lectin mutations, antibody libraries, and peptide libraries are beneficial sources. We have so far identified carbohydrate-binding molecules, regardless of natural sequences. We previously identified GM1-binding pentadecapeptides (15-mer peptides) from a random peptide library, one of which, p3, was specific to GM1 with a K_d of 1.2 μM (*25*, *26*). This peptide exhibited unique recognition, including specific binding of the high-density GM1 domain. NMR analyses indicated that p3 underwent a conformational change on binding to GM1 (induced fit) (*27*). N-Terminal and C-terminal residues of p3 are flexible in the free state but are restricted once the carbohydrate−peptide interaction occurs. The energy of this binding could be used to overcome the entropy cost for this change. If the peptide conformation is rigid, no binding energy would have to be expended to pay the cost of this folding. We